SYNTHESIS AND CHARACTERIZATION OF POLYPYRROLE/
MONTMORILLONITE AND POLYPYRROLE/
POLYPROPYLENE COMPOSITES

A THESIS SUBMITTED TO
THE GRADUATE SCHOOL OF NATURAL AND APPLIED SCIENCES
OF
MIDDLE EAST TECHNICAL UNIVERSITY

BY

ÇETİN BÖRÜBAN

IN PARTIAL FULFILLMENT OF THE REQUIREMENTS
FOR
THE DEGREE OF MASTER OF SCIENCE
IN
POLYMER SCIENCE AND TECHNOLOGY

JULY 2007

Approval of the thesis:

SYNTHESIS AND CHARACTERIZATION OF POLYPYRROLE/MONTMORILLONITE AND POLYPYRROLE/POLYPROPYLENE COMPOSITES

submitted by **ÇETİN BÖRÜBAN** in partial fulfillment of the requirements for the degree of **Master of Science in Polymer Science And Technology Department, Middle East Technical University** by,

Prof. Dr. Canan Özgen
Dean, Graduate School of **Natural and Applied Sciences**   _____

Assoc. Prof.Göknur Bayram
Head of Department, **Polymer Science and Technology**   _____

Prof. Dr. Zuhal Küçükyavuz
Supervisor, **Chemistry Department, METU**   _____

Examining Committee Members:

Prof. Dr. Nesrin Hasırcı
Chemistry Department, METU   _____

Prof. Dr.Zuhal Küçükyavuz
Chemistry Department, METU   _____

Prof. Dr. Güngör Gündüz
Chemical Engineering Department, METU   _____

Assist. Prof. Dr.Ayşen Yılmaz
Chemistry Department, METU   _____

Assist. Prof. Dr. Nurdan Sankır
Physics Department, TOBB-ETU   _____

Date: _____

I hereby declare that all information in this document has been obtained and presented in accordance with academic rules and ethical conduct. I also declare that, as required by these rules and conduct, I have fully cited and referenced all material and results that are not original to this work.

Name, Last Name: Çetin Börüban

Signature:

ABSTRACT

SYNTHESIS AND CHARACTERIZATION OF POLYPYRROLE/ MONTMORILLONITE AND POLYPYRROLE/ POLYPROPYLENE COMPOSITES

Börüban, Çetin

M.S. Department of Polymer Science and Technology

Supervisor: Prof. Dr. Zuhal Küçükyavuz

July 2007, 75 pages

In this study, organo-montmorillonite (OMMT) nanocomposites containing 1%, 5%, 10% and 15% OMMT were prepared by in *situ* intercalative oxidative polymerization of pyrrole in the presence of OMMT. Thermal and morphological properties of the Polypyrrole(PPy)/OMMT nanocomposites were investigated by Thermal Gravimetric Analysis (TGA), X-ray Diffraction Analysis (XRD) and Scanning Electron Microscope (SEM). Electrical conductivities of composites were measured by four probe technique.

Formation of PPy and its incorporation in PPy/OMMT composites were confirmed by FTIR analysis. TGA results showed that PPy/OMMT composites have outstanding thermal stability compared to that of PPy. XRD analysis revealed intercalation of PPy in the OMMT lamelles. Scanning electron micrographs demonstrated that the morphology of the PPy/OMMT nanocomposites differ slightly from that of the clay, since the modification of PPy was not significant in

flaky structure of OMMT nanoparticles. Conductivity values of PPy/OMMT composites were found in the order of 10^{-3}S/cm.

Since PPy has poor processibility, Polypropylene(PP)/PPy composites were prepared in the composition range of 2-20 % PPy. Mechanical properties were investigated by tensile tests. Electrical conductivities were measured by four probe technique. Morphological characterizations were made by SEM.

Young's Modulus of PPy/PP composites increased with increasing PPy content, and addition of 2 wt % PPy to PP resulted in a dramatic decrease in the tensile strain at break of the material. Also by addition of 2 wt % PPy to PP, the tensile strength of material decreased and further increase in PPy content, tensile strength increased. Furthermore, an increase in the PPy content in PPy/PP composites resulted in an increase in conductivity. SEM micrographs revealed that as the PPy loading increases from 10% to 20% in composite system, adhered PPy particles by PP matrix were driven out of PP matrix while PP matrix oriented along the draw direction during tensile test.

Keywords: Polypyrrole, Montmorillonite, Polypropylene/polypyrrole composites, Nanocomposite

ÖZ

POLİPİROL/MONTMORİLLONİT VE POLİPİROL/POLİPROPİLEN KOMPOZİTLERİNİN SENTEZİ VE KARAKTERİZASYONU

Börüban, Çetin

Yüksek Lisans, Polimer Bilimi ve Teknolojisi Bölümü
Tez Yöneticisi: Prof. Dr. Zuhal Küçükyavuz

Temmuz 2007, 75 sayfa

Bu çalışmada, 1%, 5%, 10% and 15% organo-montmorillonit (OMMT) içeren OMMT nanokompozitleri üretildi. Kompozitler, pirol'ün OMMT' nin bulunduğu ortamda *in situ* interkalativ oksidatif polimerizasyonu ile hazırlandı. PPy/OMMT nanokompozitlerinin ısıl özellikleri Termal Gravimetrik Analiz (TGA) yöntemi ile incelendi. Morfolojik özellikler, X-ışını difraksiyonu (XRD) ve Taramalı Elektron Mikroskobu (SEM) kullanılarak incelendi. Elektriksel iletkenlikleri dört nokta yöntemiyle ölçüldü. PPy polimerinin oluştuğu ve PPy/OMMT kompozit yapısına girdiği FTIR analizi ile doğrulandı. TGA sonuçları PPy/OMMT kompozitlerinin ısıl olarak saf polipirolden çok daha dayanıklı olduğunu göstermiştir. XRD analizleri, polipirolün OMMT düzlemleri arasına yerleştiğini ispatlamıştır. Taramalı elektron mikrografikleri, PPy/OMMT kompozitlerinin morfolojilerinin OMMT'nin morfolojisin den farklı olduğunu göstermiştir. Çünkü PPy, OMMT nanoparçacıklarının ince tabakalı yapısını değiştirmiştir. PPy/OMMT kompozitlerinin iletkenlik değerleri 10^{-3} S/cm mertebesindedir.

Saf PPy işlenebilir bir polimer olmadığından, hem iletken hem de işlenebilir bir malzeme elde etmek için, polipirolün termoplastik olan polipropilen ile birleşimi 2-20% aralığında değişen kompozitler hazırlanmıştır. Kompozitlerin mekanik özellikleri uzama testleri ile incelenmiştir. Elektriksel iletkenlikleri dört nokta yöntemi ile ölçülmüştür. Morfolojik özelliklerine SEM ile bakılmıştır. Mekanik testlerin sonuçları, PPy yüzdesi arttıkça PPy/PP kompozitlerinin Young modüllerinin arttığını göstermiştir. Polipropilene ağırlıkça %2 PPy eklendiğinde, kopmadaki uzamada büyük bir düşü gözlenmiştir. Yine PP'e, ağırlıkça %2 PPy eklendiğinde, kompozitlerin gerilme dayanıklılığında ani bir düşüş gözlenmiş, ancak PPy mitarının daha çok artması ile gerilme dayanıklılığı artmıştır. Ayrıca, PPy/PP kompozitlerinin iletkenlikleri PPy miktarı ile orantılı olarak artmaktadır. SEM mikrografikleri kompozit içindeki PPy miktarının %10 dan %20 e kadar arttırıldığında, polipropilen tarafından sarmalanmış PPy parçacıklarının örgüden koparıldığını ve PP matriksinin çekme yönünde uzadığını göstermektedir.

Anahtar sözcükler: Polipirol, Montmorillonit, Polipropilen/polipirol kompozitleri, Nanokompozit

To My Family

ACKNOWLEDGEMENTS

TABLE OF CONTENTS

LIST OF TABLES

LIST OF FIGURES

LIST OF ABBREVIATIONS

ASTM   American Society for Testing and Materials

CB   Conduction Band

CCC   Carbon-Carbon Composites

CMC   Ceramic Matrix Composites

CP   Conducting Polymer

FTIR   Fourier Transform Infrared Spectrometer

HDPE   High Density Poylethylene

HOMO   Highest Occupied Molecular Orbital

IMC   Inter-Metallic Composites

LUMO   Lowest Occupied Molecular Orbital

MMC   Metal Matrix Composites

MMT   Montmorillonite

OMMT   Organo-Montmorillonite

PAn   Polyaniline

PET   Polyethylene Terephthalate

PLS   Polymer Layered Silicate

PMC   Polymer Matrix Composites

PP   Polypropylene

PPNA   Polypyrrole/clay Nanocomposite

PPP   Poly(p-phenylene)

PPS   Poly(paraphenylene sulphide)

PPy   Polypyrrole

PPV   Poly(pphenylene vinylene)

PTh   Polythiophene

PVAc   Poly(vinyl acetate)

Py   Pyrrole

SEM   Scanning Electron Microscope

SPANI   Sulfonated Polyaniline

TEM	Transmission Electron Microscope
TGA	Thermal Gravimetric Analysis
VB	Valance Band
V_2O_5	Vanadium penta Oxide
XPS	X-ray photoelectron spectroscopy
XRD	X-Ray Diffraction
Y_2O_3	Yttrium Oxide

CHAPTER 1

INTRODUCTION

1.1 History of Conducting Polymers

Although most semiconductors are of inorganic nature, it has long been known that conjugated organic molecules may exhibit semiconductor behavior. These structures can be present in polymers, and, as a consequence of the specific properties of these materials, such as high flexibility, high impact resistance, and low density, which make them specially attractive, efforts have been devoted to the preparation of conducting polymers [1]. The term conjugated polymer defines a backbone chain that is unsaturated and therefore has alternating double and single bonds along the chain, all carbon atoms are singly bonded to neighboring carbon atoms and remaining valence electrons are bound to hydrogen atoms. Conjugated polymers can be converted into metals by doping and therefore form new class of materials referred as synthetic metals, or conducting polymers [2]. Since their discovery in the mid-1970s, conducting polymers have been a hot research area for many academic institutions [3].

Polyaniline is one of the oldest known conductive polymers, which was first prepared by Letheby in 1862. He oxidized aniline anodically in sulphuric acid and described the existence of polymer in four different states, each of which was an octamer [4]. In 1971, H. Shirakawa and S.Ikeda discovered that polyacetylene (PA) can be made into films having metallic luster and low-level conductivity. However, the field of conductive polymers really began in 1977, when A.J. MacDiarmid and

A.J. Heeger found that doping of polyacetylene with iodide demonstrated a much higher conductivity than with other dopants, with conductivities reaching as high as 10^6 Scm^{-1} under approprite conditions [2]. A.J. Heeger, A.J. MacDiarmid, and Hideki Shirakawa were rewarded for their primary work the 2000 Nobel Prize in Chemistry [5].

It was further found that polyacetylene could be obtained by both oxidative and reductive polymerization. Its conductivity depended on the doping ion's properties and concentration. Dopants reduce or oxidize the polymer to form p-type and n-type conductors [6]. Despite high conductivity of polyacetylene film in doped form, the material was inprocessible since it was unstable in air and insoluble in solvents. Synthetic work focused on increasing the processibility of (PA) by means of increasing its stability and solubility [5]. Unfortunately, the electrical conductivities of the PA derivatives were much lower than the conductivity of PA. Naturally, much work has been devoted to develop stable and processable conducting polymer structures [7].
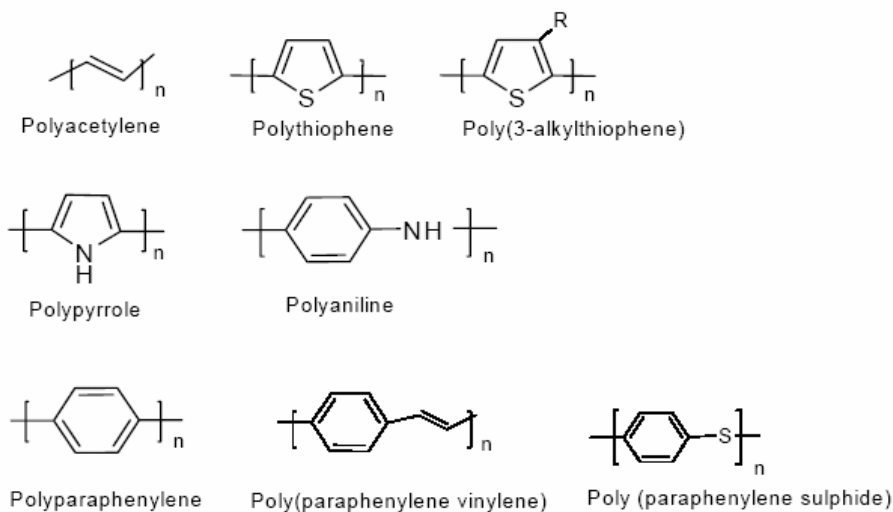
Figure 1.1 Structures of several conducting polymers

In 1980's polyheterocyles (Figure 1.1), which were more air stable than polyacetylene, due to lower polymer oxidation potential, were first developed. New classes of conducting polymers include polythiophene (PTh), polypyrrole (PPy), poly(p-phenylene) (PPP), poly(p-phenylene vinylene) (PPV), poly(paraphenylene sulphide) (PPS) and polyaniline (PAn). In Table 1.1 conductivities and stabilities of some of these polymers were shown.

Table 1.1 Conductivities and stabilities of some polymers

Derivatives of	Conductivity (S/cm)	Stability (doped state)
Polyacetylene	10^3-10^5	Poor
Polypyrrole	100	Good
Polythiophene	100	Good
Polyaniline	10	Good
Polyphenylene	1000	Poor

1.2. Applications of Conducting Polymers

There are two main groups of applications for conducting polymers. The first group utilizes their conductivity as its main property. The second group utilizes their electroactivity. The extended π-systems of conjugated polymer are highly susceptible to chemical or electrochemical oxidation or reduction. These alter the electrical and optical properties of the polymer, and by controlling this oxidation and reduction, it is possible to precisely control these properties. Since these reactions are often reversible, it is possible to systematically control the electrical

and optical properties with a great deal of precision. It is even possible to switch from a conducting state to an insulating state [8].

1.2.1. Applications that utilizes conductivity

These applications uses just the polymer's conductivity. The polymers are used because of their light weight, biological compatibility for ease of manufacturing and low cost.

By coating an insulator with a very thin layer of conducting polymer it is possible to prevent the buildup of static electricity. This is particularly important where such a discharge is undesirable. Such a discharge can be dangerous in an environment with flammable gasses and liquids and also in the explosives industry. In the computer industry the sudden discharge of static electricity can damage microcircuits. This has become particularly acute in recent years with the development of modern integrated circuits. To increase speed and reduce power consumption, junctions and connecting lines are finer and closer together. The resulting integrated circuits are more sensitive and can be easily damaged by static discharge at a very low voltage. By modifying the thermoplastic used by adding a conducting plastic into the resin results in a plastic that can be used for the protection against electrostatic discharge.

By placing monomer between two conducting surfaces and allowing it to polymerise it is possible to stick them together. This is a conductive adhesive and is used to stick conducting objects together and allow an electric current to pass through them.

Many electrical devices, particularly computers, generate electromagnetic radiation, often radio and microwave frequencies. This can cause malfunctions in nearby electrical devices. The plastic casing used in many of these devices are transparent to such radiation. By coating the inside of the plastic casing with a conductive surface this radiation can be absorbed. This can best be achieved by using conducting plastics. This is cheap, easy to apply and can be used with a wide range

4

of resins. The final finish generally has good adhesion, gives a good coverage, thermally expands approximately the same as the polymer it is coating, needs just one step and gives a good thickness [8].

Many electrical appliances use printed circuit boards. These are copper coated epoxy-resins. The copper is selectively etched to produce conducting lines used to connect various devices. These devices are placed in holes cut into the resin. In order to get a good connection the holes need to be lined with a conductor. Copper has been used but the coating method, electroless copper plating, has several problems. It is a multistage process, the copper plating is not very selective and the adhesion is generally poor. This process is being replaced by the polymerisation of a conducting plastic. If the board is etched with potassium permanganate solution a thin layer of manganese dioxide is produced only on the surface of the resin. This will then initiate polymerisation of a suitable monomer to produce a layer of conducting polymer. This is much cheaper, easy and quick to do, is very selective and has good adhesion [9].

Due to the biocompatability of some conducting polymers they may be used to transport small electrical signals through the body, i.e. act as artificial nerves. Perhaps modifications to the brain might eventually be contemplated [10].

Weight is at a premium for aircraft and spacecraft. The use of polymers with a density of about 1 gcm^{-3} rather than 10 gcm^{-3} for metals is attractive. Moreover, the power ratio of the internal combustion engine is about 676.6 watts per kg. This compares to 33.8 watts per kg for a battery-electric motor combination. A drop in magnitude of weight could give similar ratios to the internal combustion engine [10]. Modern planes are often made with light weight composites. This makes them vulnerable to damage from lighting bolts. By coating aircraft with a conducting polymer the electricity can be directed away from the vulnerable internals of the aircraft.

Molecular electronics are electronic structures assembled atom by atom. One proposal for this method involves conducting polymers. A possible example is a

modified polyacetylene with an electron accepting group at one end and a withdrawing group at the other. A short section of the chain is saturated in order to decouple the functional groups. This section is known as a 'spacer' or a 'modulable barrier'. This can be used to create a logic device. There are two inputs, one light pulse which excites one end and another which excites the modulable barrier. There is one output, a light pulse to see if the other end has become excited. To use this there must be a great deal of redundancy to compensate for switching 'errors' [11].

1.2.2 Applications that utilizes electroactivity

Depending on the conducting polymer chosen, the doped and undoped states can be either colourless or intensely coloured. However, the colour of the doped state is greatly redshifted from that of the undoped state. The colour of this state can be altered by using dopant ions that absorb in visible light. Because conducting polymers are intensely coloured, only a very thin layer is required for devices with a high contrast and large viewing angle. Unlike liquid crystal displays, the image formed by redox of a conducting polymer can have a high stability even in the absence of an applied field. The switching time achieved with such systems has been as low as 100 μs but a time of about 2 ms is more common. The cycle lifetime is generally about 10^6 cycles. Experiments are being done to try to increase cycle lifetime to above 10^7 cycles [11].

The chemical properties of conducting polymers make them very useful for use in sensors. This utilizes the ability of such materials to change their electrical properties during reaction with various redox agents (dopants) or via their instability to moisture and heat. An example of this is the development of gas sensors. It has been shown that polypyrrole behaves as a quasi 'p' type material. Its resistance increases in the presence of a reducing gas such as ammonia, and decreases in the presence of an oxidizing gas such as nitrogen dioxide. The gases cause a change in the near surface charge carrier (here electron holes) density by reacting with surface adsorbed oxygen ions [10]. Another type of sensor developed is abiosensor. This utilizes the ability of triiodide to oxidize polyacetylene as a

6

means to measure glucose concentration. Glucose is oxidized with oxygen with the help of glucose oxidase. This produces hydrogen peroxide which oxidizes iodide ions to form triiodide ions. Hence, conductivity is proportional to the peroxide concentration which is proportional to the glucose concentration.

Probably the most publicized and promising of the current applications are light weight rechargeable batteries. Some prototype cells are comparable to, or better than nickel-cadmium cells now on the market. The polymer battery, such as a polypyrrole-lithium cell operates by the oxidation and reduction of the polymer backbone. During charging the polymer oxidizes anions in the electrolyte enter the porous polymer to balance the charge created. Simultaneously, lithium ions in electrolyte are electrodeposited at the lithium surface. During discharging electrons are removed from the lithium, causing lithium ions to reenter the electrolyte and to pass through the load and into the oxidized polymer. The positive sites on the polymer are reduced, releasing the charge-balancing anions back to the electrolyte. This process can be repeated about as often as a typical secondary battery cell [8].

Conducting polymers can be used to directly convert electrical energy into mechanical energy. This utilizes large changes in size undergone during the doping and dedoping of many conducting polymers. This can be as large as 10%. Electrochemical actuators can function by using changes in a dimension of a conducting polymer, changes in the relative dimensions of a conducting polymer and a counter electrode and changes in total volume of a conducting polymer electrode, electrolyte and counter electrode. The method of doping and dedoping is very similar as that used in rechargeable batteries discussed above. What is required are the anodic strip and the cathodic strip changing size at different rates during charging and discharging. The applications of this include microtweezers, microvalves, micropositioners for microscopic optical elements, and actuators for micromechanical sorting (such as the sorting of biological cells).

One of the most futuristic applications for conducting polymers are 'smart' structures. These are items which alter themselves to make themselves better. An example is a golf club which adapt in real time to a persons tendency to slice or

undercut their shots. A more realizable application is vibration control. Smart skis have recently been developed which do not vibrate during skiing. This is achieved by using the force of the vibration to apply a force opposite to the vibration. Other applications of smart structures include active suspension systems on cars, trucks and train; traffic control in tunnels and on roads and bridges; damage assessment on boats; automatic damping of buildings and programmable floors for robotics [11].

1.3 Conduction mechanisms

1.3.1 Band Theory

The electrical conductivities of materials allow them to be classified into three groups called conductors, semiconductors and insulators. In polymeric materials conduction may occur through the movement of either electrons or ions. In both cases electrical conductivity depends on a number of fundamental parameters, such as the number density of mobile charge carriers n, the charge q, and the carrier mobility μ. The relationship between conductivity and the three latter quantities is expressed by the general relationship [12].

$$\sigma = n\, q\, \mu$$

The conduction mechanism can be explained by using the band theory, which explains the electronic structure of materials, as shown in Figure 1.2. The highest occupied bands are the valance band (VB) and the lowest unoccupied bands are the conduction band (CB). The energy spacing between the highest occupied molecular orbital (HOMO) and the lowest occupied molecular orbital (LUMO) is known as band gap energy (E_g). For metals the VB and CB overlap and the intrinsic conductivity is attributed to the zero band gap. For semi-conductors, the narrow band gap energy enables the electrons to jump to CB by thermal excitation even at room temperature to render the material conductive. Materials where the energy separation is too large for thermal excitation to promote electrons to CB are termed as insulators [13].
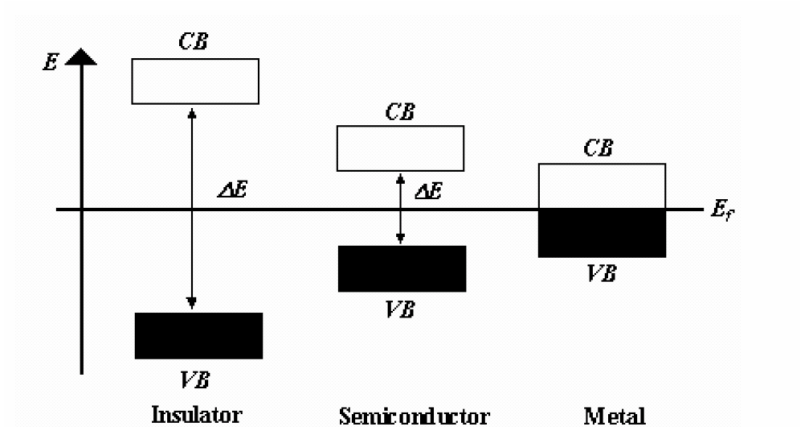
Figure 1.2 Schematic representation of a band structure of a metal,   semiconductor and an insulator

1.3.2 Doping Process of Conducting Polymers

The concept of doping is the unique, central, underlying, and unifying theme which distinguishes conducting polymers from all other types of polymers. During the doping process, an organic polymer, either an insulator or semiconductor having a small conductivity, typically in the range 10^{-10} to 10^{-5} Scm^{-1}, is converted into a polymer which is in the "metallic" conducting regime (ca. 1 to 10^{4} Scm^{-1}). The controlled addition of known, usually small ($\leq$10%) nonstoichiometric quantities of chemical species results in dramatic changes in the electronic, electrical, magnetic, optical, and structural properties of the polymer. Doping is reversible to produce the original polymer with little or no degradation of the polymer backbone. Both doping and undoping processes, involving dopant counterions which stabilize the doped state, may be carried out chemically or electrochemically.[14]

All conducting polymers undergo either p- and/or n-redox doping by chemical and/or electrochemical processes during which the number of electrons associated with the polymer backbone changes [15,16].

9

p-Doping, that is, partial oxidation of the π backbone of an organic polymer, was first discovered by treating trans-$(CH)_x$ with an oxidizing agent such as iodine[17,18].

$$trans\text{-}(CH)_x + 1.5xyI_2 \rightarrow [CH^{+y}(I_3)_y^-]_x \quad (y \leq 0.07)$$
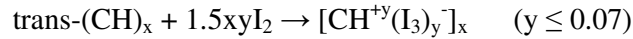
This process was accompanied by an increase in conductivity from ca. 10^{-5} Scm^{-1} to ca. 10^3 Scm^{-1}. If the polymer is stretch-oriented five- to six-fold before doping, conductivities parallel to the direction of stretching up to around 10^5 Scm^{-1} can be obtained [15,16].

n-Doping, that is, partial reduction of the backbone π system of an organic polymer, was also discovered using trans-$(CH)_x$ by treating it with a reducing agent such as liquid sodium amalgam or preferably sodium naphthaline. (Nphth = naphthaline)

$$trans\text{-}(CH)_x + (xy)Na^+(Nphth)^- \rightarrow [Na_y^+ (CH)^{-y}]_x + Nphth \quad (y \leq 0.1)$$
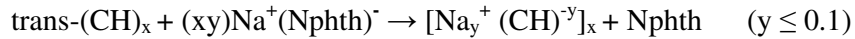
The antibonding π system is partially populated by this process which is accompanied by an increase in conductivity of about 10^3 Scm^{-1} [17,18].

1.3.3 Polaron and Bipolaron Model

The conventional doping process in the semiconductor generates intermediate energy levels within the band gap and these mid-gap states exist as either a hole for p doping or electrons for n doping. Either holes or electrons contribute to the electrical conductivity of semiconductors, as charge carriers. A conducting polymer is known as an organic semiconductor whose band gap is usually above 1.5 eV and whose intrinsic conductivity is low. Doping (oxidation or reduction in chemistry terms) is necessary to produce higher conductivity [19].

The polaron-bipolaron model has been widely applied to conjugated polyheterocyclic material. The concepts of polaron and bipolaron are from solid-

state physics. From the chemistry point of view a polaron is a radical cation that stabilizes itself by polarizing. Considering polypyrrole (Figure 1.3) as an example, upon the oxidative doping of polypyrrole, an electron is removed from the p-orbital of the backbone producing a free radical and a spinless positive charge. The combination of a charge site and a radical is called a polaron, which has a spin of 1/2. This creates new localized electronic states in the band gap, with the lower energy states being occupied by single unpaired electrons. The polaron state of polypyrrole is symmetrically located about 0.5 eV from the band edges. The partial delocalization of polaron across several monomeric units leads to structural distortion in the polymer. The distortion is caused by the existence of two nondegenerate ground states, namely aromatic and quinoid. Upon further oxidation, the free radical of the polaron is removed, creating a new spinless defect called a bipolaron. This is of lower energy than the creation of two distinct polarons. At higher doping levels it becomes possible that two polarons combine to form a bipolaron. Thus at higher doping levels the polarons are replaced with bipolarons. The bipolarons are located symmetrically with a band gap of 0.75 eV for polypyrrole. Theoretical studies have proved that the formation of bipolarons via the combination of polarons is energetically favorable eventually, leading to continuous bipolaron band with continued doping. Their band gap also increases as newly formed bipolarons are made at the expense of the band edges. For a very heavily doped polymer it is conceivable that the upper and the lower bipolaron bands will merge with the conduction and the valence bands respectively to produce partially filled bands and metallic like conductivity [20]. This is shown in Figure 1.4.
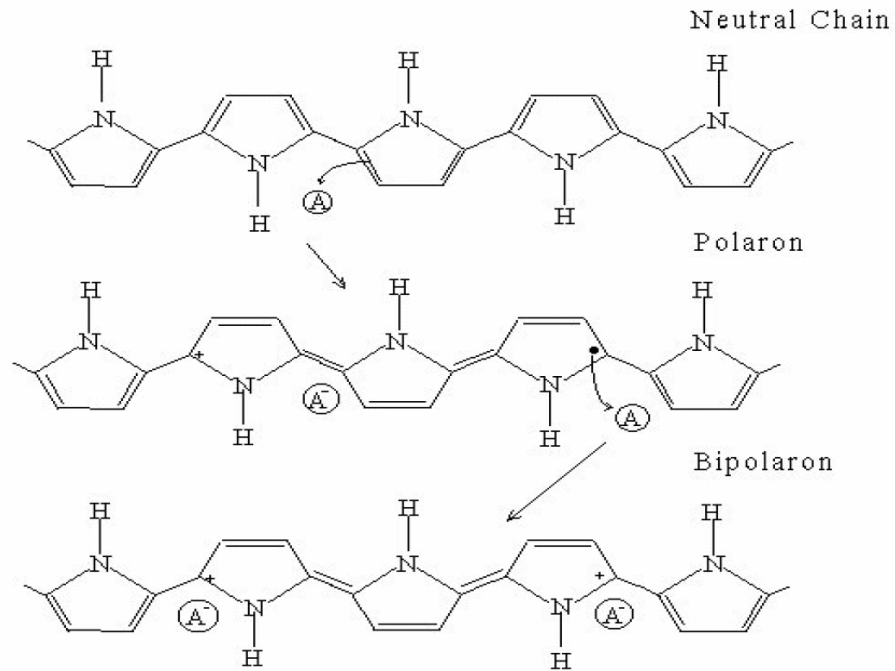
Figure 1.3 The oxidative doping of polypyrrole
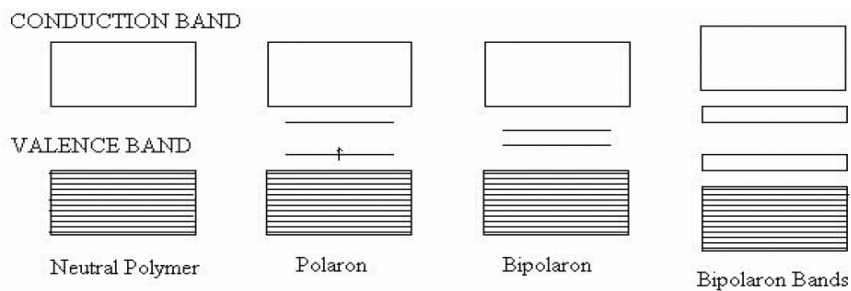
Figure 1.4 Band theory of conjugated polymers

Conductivity of CPs can be tuned over eight or more orders of magnitude in the same material. The doping level of conducting polymers affects range of

12

conductivity from insulator to metal. Fig 1.5 shows the typical conductivity ranges of the three most common conducting polymers (PA, PPy, PTh).
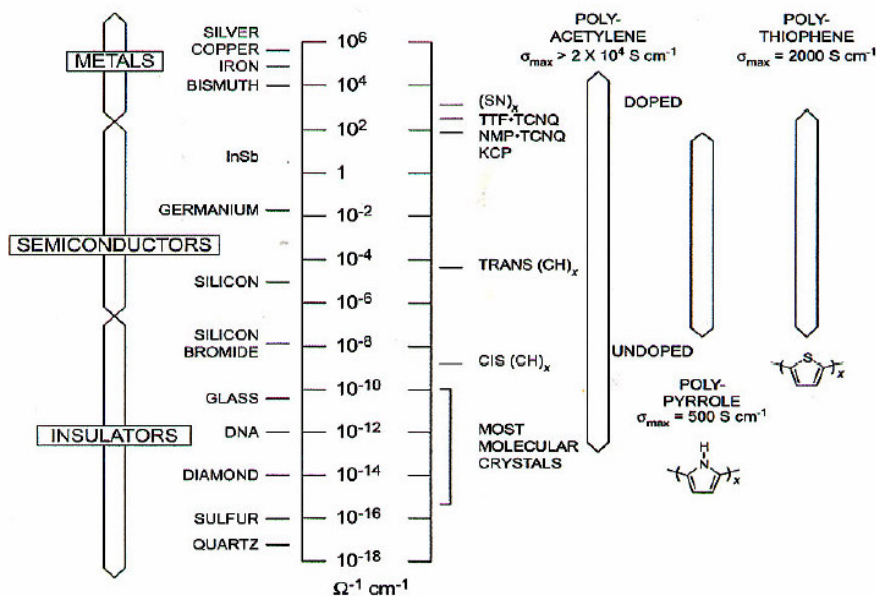
Figure 1.5 Conductivities of some metals, semiconductors and insulators

1.3.4 Hopping process

Intramolecular transport, intermolecular transport and interparticle contact determine the overall conductivity in a polymer. Latter two are known as hopping process through which transport of a particle occurs as the electronic states become increasingly localised. Among the others, interparticle contact has the greatest importance in terms of conductivity of polymers [21]

1.4 Composites

Composites are combinations of two materials in which one of the materials, called the reinforcing phase, is in the form of fibers, sheets, or particles, and is embedded in the other materials called the matrix phase. The reinforcing material and the

13

matrix material can be metal, ceramic, or polymer. Typically, reinforcing materials are strong with low densities while the matrix is usually a ductile, or tough, material. If the composite is designed and fabricated correctly, it combines the strength of the reinforcement with the toughness of the matrix to achieve a combination of desirable properties not available in any single conventional material.

For the matrix, many modern composites use **thermosetting** or **thermosoftening** plastics (also called resins). The plastics are polymers that hold the reinforcement together and help to determine the physical properties of the end product.

Thermosetting plastics are liquid when prepared but harden and become rigid (ie, they *cure*) when they are heated. The setting process is irreversible, so that these materials do not become soft under high temperatures. These plastics also resist wear and attack by chemicals making them very durable, even when exposed to extreme environments.

Thermosoftening plastics, as the name implies, are hard at low temperatures but soften when they are heated. Although they are less commonly used than thermosetting plastics they do have some advantages, such as greater fracture toughness, long shelf life of the raw material, capacity for recycling and a cleaner, safer workplace because organic solvents are not needed for the hardening process.

Ceramics, carbon and metals are used as the matrix for some highly specialised purposes. For example, ceramics are used when the material is going to be exposed to high temperatures (eg, heat exchangers) and carbon is used for products that are exposed to friction and wear [22].

1.4.1 Polymer Matrix Composites

The major classes of structural composites that exist today can be categorized as polymer matrix composites (PMC), metal matrix composites (MMC), ceramic matrix composites (CMC), carbon-carbon composites (CCC), intermetallic

composites (IMC) or hybrid composites. PMC are the most developed class of composite materials in that they have found widespread application, can be fabricated into large, complex shapes, and have been accepted in a variety of aerospace and commercial applications. They are constructed of components such as carbon or boron fibers bound together by an organic polymer matrix. These reinforced plastics are a synergistic combination of high-performance fibers and matrices. The fiber provides the high strength and modulus, whereas the matrix spreads the load as well as offering resistance to weathering and corrosion. Composite strength is almost directly proportional to the basic fiber strength and can be improved at the expense of stiffness. High modulus organic fibers have been made with simple polymers by arranging the molecules during processing, which results in a straightened molecular structure [23].

1.5 Nanocomposites

The definition of nanocomposite material has broadened significantly to encompass a large variety of systems such as one-dimensional, two-dimensional, three-dimensional and amorphous materials, made of distinctly dissimilar components and mixed at the nanometer scale (10^{-9} nm). The general class of nanocomposite organic/inorganic materials is a fast growing area of research [24]. Major differences in behavior between conventional composites and nanocomposites result from the fact that the latter have much larger interface area per unit volume leading to unique phase morphology [25].

This rapidly expanding field is generating many exciting new materials with novel properties. The latter can derive by combining properties from the parent constituents into a single material. There is also the possibility of new properties which are unknown in the parent constituent materials.

The inorganic components can be three-dimensional framework systems such as zeolites, two-dimensional layered materials such as clays, metal oxides, metal phosphates, chalcogenides, and even one-dimensional and zero-dimensional

materials such as $(Mo_3Se_3-)_n$ chains and clusters. Experimental work has generally shown that virtually all types and classes of nanocomposite materials lead to new and improved properties when compared to their macrocomposite counterparts. Therefore, nanocomposites promise new applications in many fields such as mechanically reinforced lightweight components, non-linear optics, battery cathodes and ionics, nano-wires, sensors and other systems [26].

1.6 Clays

The clay minerals are a part of a general but important group within the phyllosilicates (Figure1.6) that contain large percentages of water trapped between the silicate sheets. Most clays are chemically and structurally analogous to other phyllosilicates but contain varying amounts of water and allow more substitution of their cations. There are many important uses and considerations of clay minerals. They are used in manufacturing, drilling, construction and paper production. They have geat importance to crop production as clays are a significant component of soils [27].

Common clays are naturally occurring minerals and are thus subject to natural variability in their constitution. The purity of the clay can affect final nanocomposite properties. Many clays are aluminosilicates, which have a sheet-like (layered) structure, and consist of silica SiO_4 tetrahedra bonded to alumina AlO_6 octahedra in a variety of ways. A 2:1 ratio of the tetrahedra to the octahedra results in smectite clays, the most common of which is montmorillonite. Other metals such as magnesium may replace the aluminium in the crystal structure.
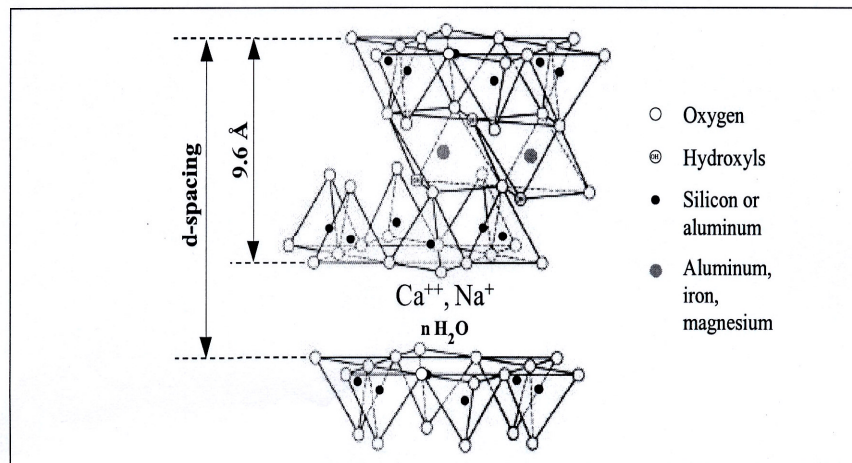
Figure 1.6 Structure of 2:1 phyllosilicates

Depending on the precise chemical composition of the clay, the sheets bear a charge on the surface and edges, this charge being balanced by counter-ions, which reside in part in the inter-layer spacing of the clay. The thickness of the layers (platelets) is of the order of 1 nm and aspect ratios are high, typically 100-1500 nm. The clay platelets are truly nanoparticulate. In the context of nanocomposites, it is important to note that the molecular weight of the platelets (ca. 1.3×10^8) is considerably greater than that of typical commercial polymers, a feature which is often misrepresented in schematic diagrams of clay-based nanocomposites. In addition, platelets are not totally rigid, but have a degree of flexibility. The clays often have very high surface areas, up to hundreds of m^2 per gram. The clays are also characterised by their ion (e.g. cation) exchange capacities, which can vary widely. One important consequence of the charged nature of the clays is that they are generally highly hydrophilic species and therefore naturally incompatible with a wide range of polymer types [28]. The interactions between organic matter and clay minerals are among the the most widespread reactions in nature. The adsorption of organic materials by clay minerals has been widely investigated during the last decade and has been extensively reviewed. The interactions include cation exchange and adsorption of polar and nonpolar molecules. In these interactions,

17

adsorption, in which physicalor chemical bonds(long- or short- range interactions, respectively) are formed between the mineral and the organic matter, is the primary process. In most adsorption reactions the clay minerals serve as the substrates and the organic entities are the adsorbed species. Secondary process may follow the primary adsorption reactions: Adsorption properties of the clay minerals may be altered after primary adsorption. In their naturel form clay minerals appear with ınorganic exchangeable cations, which contribute to their hydrophilicity[29].

1.6.1 Montmorillonite

Montmorillonite is a layered silicate belonging to the smectite group of phyllosilicate minerals. It is formed primarily by the alteration of extrusive volcanic rocks such as volcanic ash falls and ash fall tuffs. Commonly these minerals are products of geological weathering or hydrothermal alteration of silicate minerals and silica phases in these igneous rocks [30]. Montmorillonite's water content is variable and it increases greatly in volume when it absorbs water. Chemically it is hydrated sodium calcium aluminium magnesium silicate hydroxide (Na, Ca)$_x$ (Al, Mg)$_2$ (Si$_4$O$_{10}$) (OH)$_2$.nH$_2$O. Potassium, iron and other cations are common substitutes, the exact ratio of cations varies with source [31].

Similar to other clays, montmorillonite swells with the addition of water. However, some montmorillonites expand considerably more than other clays due water penetrating the interlayer molecular spaces and concomitant adsorption. The amount of expansion is due largely to the type of exchangeable cation contained in the sample. The presence of sodium as the predominant exchangeable cation can result in the clay swelling to several times its original volume. Hence, sodium montmorillonite has come to be used as the major constituent in non-explosive agents for splitting rock in natural stone quarries in order to limit the amount of waste, or for the demolition of concrete structures where the use of explosive charges is unacceptable.

It is the absorption and swelling characteristics that makes montmorillonite so useful in industrial and commercial applications. Montmorillonite is used in cat litters, industrial oil absorbents, filtration media, animal feeds and agricultural applications [30].

1.7 Cation–Exchange Process

The sorptive properties of the smectite clays for organic molecules are greatly modified by replacing native exchangeable metallic cations with long-chain or quaternary ammonium cations. These modified clays are comonly referred to as 'organo-clays'. There are two different types of organoclays: Those saturated with large quaternary ammonium cations and with one or two long alkyl chains and those saturated with small quetarnery ammonium aliphatic and aromatic cations. Some investigators use the term 'organophilic-clays' for the first type and the 'adsorptive clays' for the organoclays saturated with small quatenary cations.

It is now common to synthesize organophilic clays by replacing the metallic cations by quaternary cations of the type $[(CH_3)_3NR']^+$ or $[(CH_3)_2NR'R'']^+$, where R' and R'' are aliphatic or aromatic substitutents, respectively. The adsorption of a quaternary ammonium cation by a cation exchange mechanism is independent of the pH of the system, whereas cation exchange adsorption of primary, secondary, or tertiary ammonium cation depends on the pH of the system. In addition, the quaternary ammonium cation does not show acidic or basic properties and does not form H-bonds either with proton donors or with acceptors [29].
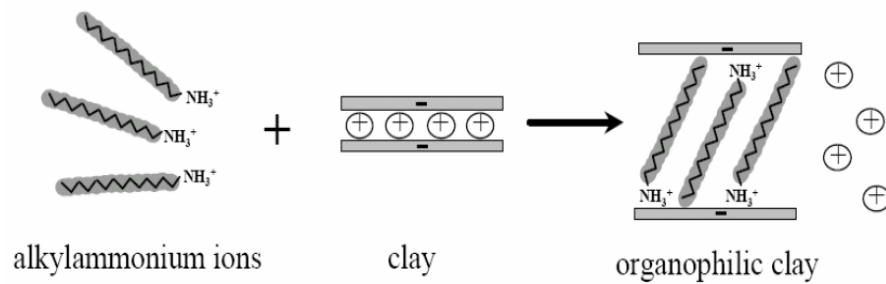
Figure 1.7 Schematic representation of the cation exchange process.

The ion-exchange process in smectite clays not only serves to match the clay surface polarity with the polarity of the polymer, but it also expands the clay galleries. In general, the longer the surfactant chain length, the further apart the clay layers will be forced [32].

1.8 Structure of PLS nanocomposites

Polymer/clay composites are divided into three general types, namely phase separated, intercalated, and delaminated or exfoliated. Illustrated structures can be seen in Figure 1.8.

1.8.1 Phase Separated Microcomposites

A third alternative is dispersion of complete clay particles (tactoids) within the polymer matrix, but this simply represents use of the clay as a microscale fillers.

1.8.2 Intercalated Nanocomposites

In the case of an intercalate, the organic component is inserted between the layers of the clay such as that the inter-layer spacing is expanded, but the layers stil bear a well defined spatial relationship to each other [28].
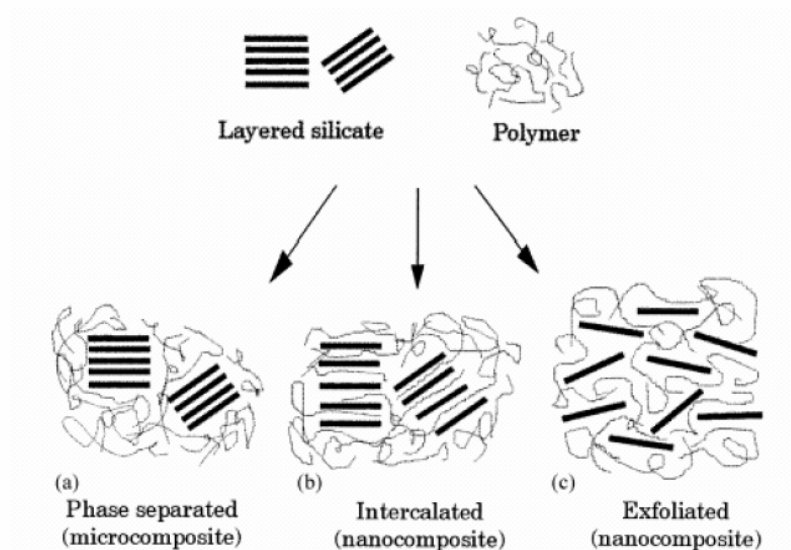
Figure 1.8 Scheme of different types of composite arising from the interaction of layered silicates and polymers: (a) phase separated microcomposite; (b) intercalated nanocomposite and (c) exfoliated nanocomposite.

1.8.3 Exfoliated Nanocomposites

In an exfoliated structure, the layers of the clay have been completely separated and the individual layers are distributed throughout the organic matrix. The silicate layers are totaly delaminated and the layers stand >100 Å apart.Usually, the clay content of an exfoliated nanocomposites is much lower than that of an intercalated nanocomposites [33].

1.9 Synthesis of PLS nanocomposites

Three main methods used for preparing PLS nanocomposites are: *In-Situ* Intercalative Polymerization Method, *Solution* Intercalation Method and *Melt* Intercalation Method.

1.9.1 In Situ Intercalative Polymerization Method

In this method, the OMMT is swollen within the liquid monomer or a monomer solution so that the polymer formation can occur in between the intercalated sheets. Polymerization can be initiated either by heat or radiation, by the diffusion of a suitable initiator, or by an organic initiator or catalyst fixed through cation exchange inside the interlayer before the swelling step by the monomer [33]. MMT may be conventionally represented as containing sorbed cations (M^{n+}) between silicate network which are co-ordinated to solvent moieties usually H_2O, the coordination number depending on the nature of the sorbed cations [34].
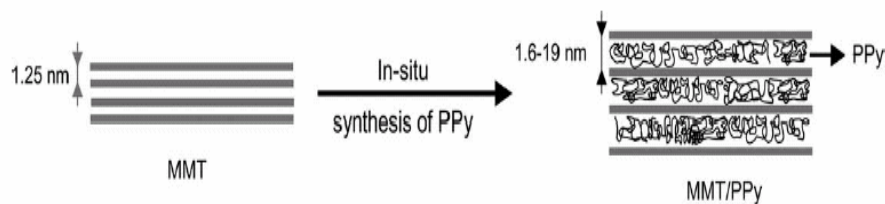
Figure 1.9 Schematic representation of polypyrrole intercalation in the MMT galleries.

1.9.2 Solution Intercalation Method

This route involves the dispersion of the organoclay and the polymer in water or polar organic solvent. The high polarity of water results in swelling of Na^+MMT. The layer silicates owing to their unique feature can be dispersed easily in an adequate solvent. The polymer dissolves in the solvent, then adsorbs onto the expanded silicate sheets. When the solvent is evaporated, the sheets reassemble, sandwiching the polymer to form the intercalated structure [35].

1.9.3 Melt Intercalation Method

This method involves annealing, statically or under shear, a mixture of the polymer and OMMT above the softening point of the polymer. Melt intercalation is broadly applicable to many commodity and engineering polymers, from non-polar polyolefin, weakly polar PET to strong polar amide. Melt compounding is a well-known process to fabricate various thermoplastics into useful shapes with low cost and high productivity. Morever, the high shear environment of the melt extruder can assist delamination or exfoliation of the clay platelets [33].

1.10 Properties of Polypyrrole

Among the conducting polymers, polypyrrole (PPy) is one of the most investigated due to its high electrical conductivity and its relatively good environmental stability and low toxicity [36]. This conductive polymer can be potentially used in batteries, supercapacitors, sensors, anhydrous electrorheological fluids, microwave shielding, and corrosion control [37]. Polypyrrole can be easily prepared from aqueous and organic solvents by both chemical and electrochemical methods [38].
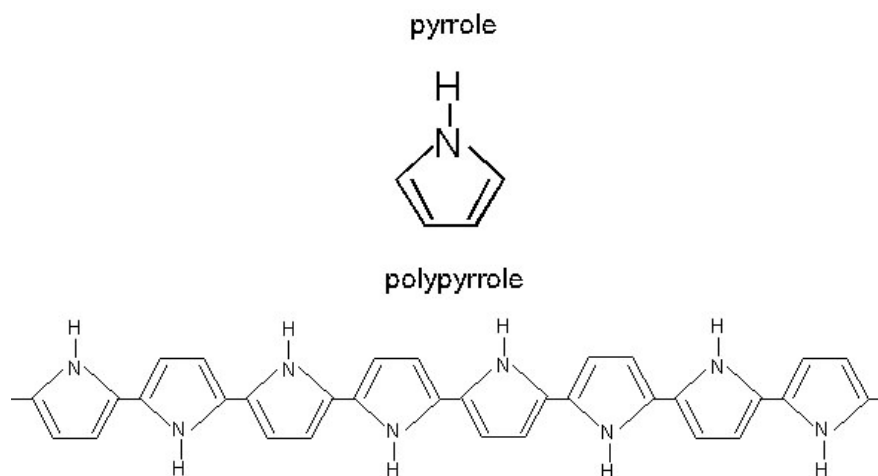
Figure 1.10 Structure of PPy

1.10.1 Synthesis of Polypyrrole

The PPy and its derivatives have been synthesized either by an electrochemical or by a chemical oxidative polymerization. Generally, PPys are brittle, insoluble and infusible, and hence inprocessible. Thereby, in order to develop PPy-based conductive materials, several approaches including oxidant-impregnated polymerization using pyrrole vapor, electrochemical polymerization of pyrrole in the presence of latex particles with anionic surface, and graft copolymerization containing pyrrole as grafted groups, have been applied [39]. These various approaches produce polypyrrole materials with different forms, chemical oxidation generally produce powders, while electrochemical synthesis leads to films dopsited on the working electrode and enzymatic polymerization gives aqueous dispersions.

Although, because of several distinct advantages, electropolymerization has been for a long period the preferred method at the laboratory scale, the recent development of solution processable PPy has triggered a strong renewal of interest in chemical polymerization, which remains the most suitable method as far as industrial production is envisioned. The electrochemical conditions, the electrode material, the solvent, the counterion and the monomer all influence the nature of the processes occuring. For example, if the applied potential is too low (under certain condition), the rate of polymerization will be such that no precipitate eventuates. If the solvent is nucleophilic (or contains dissolved oxygen), it will react with the free radical intermediates. If the electrode material is extremely polar, at the potential required for polymerization, deposition may be discouraged. In addition the solvent, monomer, counterion and substrate interactions are all important since they dictate the solubility and/or deposition of the resultant polymer.
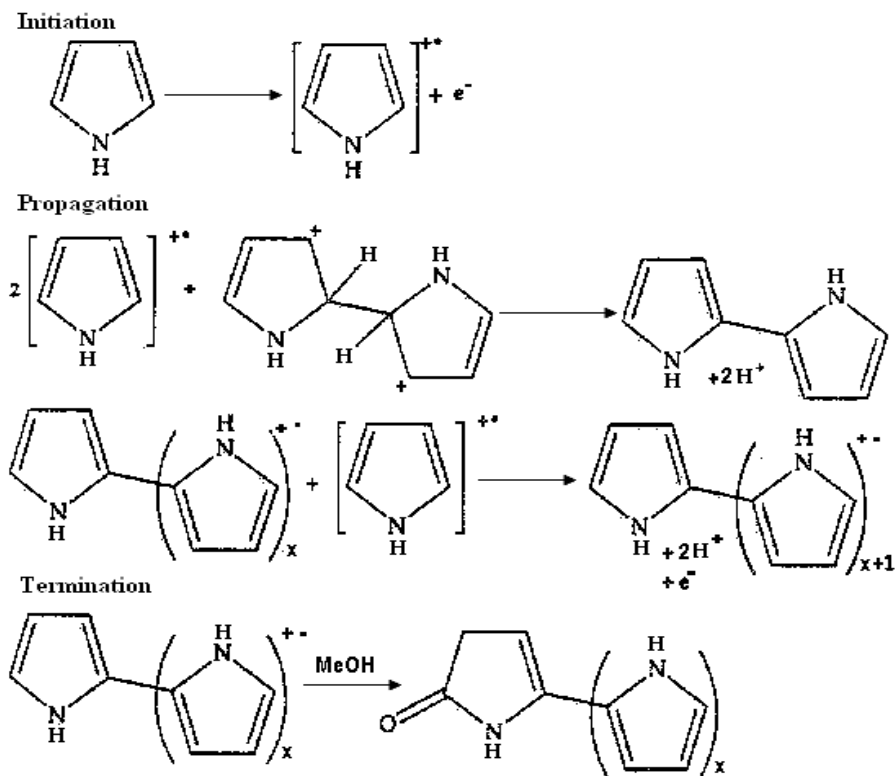
Figure 1.11 Synthesis of polypyrrole by oxidation.

The number of variables available with chemical polymerization is greatly reduced because no electrochemical cell or electrodes are employed. The range of dopant counterions that can be incorporated into the polypyrrole backbone during polymerization has also, until recently, been generally limited to ions associated with the oxidant. However, chemical polymerization remains of interest for processing purposes, first, because it may be easier to scale up this batch process, and second, it results in the formation of powders or colloidal dispersions. Furthermore, it is possible to use chemical deposition to coat other nonconducting materials [3].

1.10.2 Composites of Polypyrrole

Polypyrrole, is the subject of numerous studies due to its good environmental stability and high electrical conductivity. However, PPys are brittle, insoluble and infusible, and hence inprocessible [39]. This led to intensive research on the preparation of a variety of organic-organic and inorganic-organic polymer composites and nanocomposites [37]. The PPy and its derivatives have been synthesized either by an electrochemical or by a chemical oxidative polymerization.

Hua Bai, and Qi Chen prepared Polypyrrole/sulfonated polyaniline (PPy/SPANI) composite films by direct electrochemical polymerization of pyrrole in an aqueous solution of SPANI. Spectroscopic results demonstrated that the polyanion, SPANI, was incorporated into the PPy matrix as a dopant. The composite films exhibited a higher thermal stability than that of pure PPy. Scanning electron microscopic images revealed that the composite film had smooth and compact morphology. Furthermore, a simple ammonia sensing device based on the composite film showed high sensitivity and a low limit of detection [40].

Gaoyi Han and Gaoquan Shi prepared porous polypyrrole/polymethyl methacrylate composite films. The synthesis procedures include the vapor deposition polymerization of pyrrole on the composite films of polymethyl methacrylate and ferric hydroxide bis(1,4-bis(2-ethylhexyl) sulfosuccinate). The porous composite films showed electroactivity, and the sensors based on them exhibited high sensitivity and fast response to ammonia gas [41].

W.S. Barde, S.V. Pakade and S.P. Yawale synthesized Polypyrrole (PPy) and poly (vinyl acetate) (PVAc) composite thin films by chemical oxidative polymerization method with the solution of ferric chloride (FeCl$_3$) oxidant in methanol. Their dc conductivities as a function of temperature (308-383^0 K) were measured. The ionic transference numbers for the PPy-PVAc films, synthesized with different concentration of FeCl$_3$, were determined by dc polarization technique. The dc electrical conductivity of the films, at room temperature, first increases with

concentration of $FeCl_3$ and attains the maximum value ($r = 6.17 \times 10^{-10}$ S/cm) at 0.5 M of $FeCl_3$ [42].

Qilin Cheng, Vladimir Pavlinek and Chunzhong Li synthesized polypyrrole/nano-Y_2O_3 conducting composite by chemical oxidative polymerization. The composite was characterized using transmission electron microscopy, X-ray diffraction, FTIR spectra, X-ray photoelectron spectroscopy and electrical conductivity measurements. The results indicate that Y_2O_3 nanoparticles are almost enwrapped by polypyrrole. An interaction exists between PPy and nanocrystalline Y_2O_3, which gives rise to changes in surface properties and DC electrical conductivity of the composite, and they also improve thermal stability of the composite [43].

M.V. Murugendrappa and Ameena Parveen synthesized polypyrrole (PPy) by chemical oxidation method by using ammonium persulphate as an oxidant, and vanadium pent oxide (V_2O_5) was used as it was received. $PPy–V_2O_5$ composites were synthesized by using various weight percentages (10, 20, 30, 40 and 50) of V_2O_5 in PPy by in situ polymerization. The composites were characterized by using various techniques such as XRD, IR and SEM spectroscopy. SEM micrographs indicate that V_2O_5 was homogeneously distributed in the PPy. IR spectroscopy revealed that the characteristic stretching frequencies were shifted towards lower frequency side, as compared to pure PPy. XRD micrographs indicated that $PPy–V_2O_5$ have many aggregated pores which have been reduced due to homogeneous distribution of V_2O_5 in PPy [44].

Suprakas SinhaRay and Mukul Biswas prepared Montmorillonite (MMT)-based nanocomposites of polypyrrole (PPy) through the polymerization of pyrrole with MMT and $FeCl_3$-impregnated MMT in bulk and in aqueous medium. The composites were characterized by IR, X-ray diffraction (XRD), and scanning electron microscopy (SEM) studies. XRD analyses revealed no change in d001 spacing in MMT (9.8 Å), suggesting no intercalation of PPy into MMT lamellae. The SEM micrograph for the water-redispersible PPy-MMT nanocomposite clearly showed a highly dense agglomeration of finer spherical particles. The SEM

micrograph for the composite with high PPy loading was not particularly different from those for the composites with low PPy content. The bulk conductivity of the composites was in the range of (1.3 to 26) x 10^{-5} S/cm, depending on the $FeCl_3$-impregnation level and on the PPy loading in the composites [45].

J.W. Kim, F. Liu and H.J. Choi synthesized conducting polypyrrole (PPy) into the layer of inorganic clay within a nanolevel by an inverted emulsion pathway polymerization method, using dodecylbenzenesulfonic acid (DBSA) as both an emulsifier and a dopant. The synthesized PPy/Na^+montmorillonite (MMT) nanocomposite was confirmed to have a layered structure with a folded or penetrated PPy from X-ray diffraction, and it was further characterized via FT-IR spectroscopy. Intercalation of PPy was observed from the XRD and FT-IR analysis, in which the characteristic peaks of PPy in the polypyrrole/clay nanocomposite (PPNA) were observed. Four probes method was adopted to examine electrical DC conductivity. Since the existence of clay effects as an insulating material, the conductivity of PPNA was lower than that of pure PPy in a broad range of temperature [39].

Jui-Ming Yeh, Chih-Ping Chin and Susan Chang prepared a series of electronically conductive nanocomposite materials that consisted of soluble polypyrrole (PPy) and layered montmorillonite (MMT) clay platelets by *in situ* oxidative polymerization with dodecylbenzene sulfonic acid (DBSA) as dopant and cocamidopropylhydroxysultaine as a intercalating agent for MMT. Organic pyrrole monomers were first intercalated into the interlayer regions of organophilic clay hosts and followed by a one-step oxidative polymerization. The as-synthesized electronically conductive polypyrrole-clay nanocomposite (PCN) materials contained clay with weight ratio %1, 3%, 5% and 10%. The incorporation of nanolayers of MMT clay in electronically conductive PPy matrix resulted in a slight increase in thermal decomposition temperature based on the TGA studies. Electrical conductivity of all the PCN materials in the form of a powder-pressed pellet was found to be slightly smaller than that of pristine. XRD implied an intercalated MMT clay nanolayer structure existed in the PPy matrix [46].

28

Hong-Quan Xie, Cheng-Mei Liu and Jun-Shi Guo prepared two kinds of conductive polypyrrole composites by in-situ polymerization of pyrrole in a suspension of chlorinated polyethylene powder or in a natural rubber latex using ferric chloride as oxidizing agent. The conductivity percolation threshold of the composite is about 12%. The composites can be processed repeatedly, exhibiting a maximum tensile strength over 9 MPa and a maximum conductivity near 1 Scm^{-1}. The polypyrrole/natural rubber composites were prepared successfully by using a nonionic surfactant (Peregal O) as stabilizer at pH less than 3 with a molar ratio of $FeCl_3$/pyrrole=2.5 below 45°C. The latter composites show a low conductivity percolation threshold about 6%, a maximum tensile strength over 10 MPa and a maximum conductivity over 2 Scm^{-1} [47].

Miroslava Mravcakova and Maria Omastova prepared montmorillonite/polypyrrole (MMT/PPy) composites with two montmorillonites, an inorganic sodium montmorillonite (NaMMT) and an organo-modified montmorillonite (OMMT) which was modified with distearyldimethyl ammonium chloride, by the in situ polymerization of pyrrole in water, in aqueous solution of dodecylbenzenesulfonic acid (DBSA) used as anionic surfactant, and in water/methanol. Ferric chloride was used as oxidant in each case. Wide angle X-ray scattering patterns of OMMT/PPy composites synthesized in methanol/water showed no change in interlayer spacing and the electrical conductivity of these composites was low, similar to that of NaMMT/PPy composites prepared under the same conditions. X-ray photoelectron spectroscopy (XPS) proved that the surface of NaMMT/PPy composites is rich in MMT, whereas more PPy was found on the surface of OMMT/PPy composites [37].

1.11 Polypropylene

Polypropylene (PP) is a crystalline thermoplastic and one of the major members of the polyolefins family. It is the lightest of the widely used thermoplastics with the exception of plastic foams. With a specific gravity of less than one, polypropylene will float on water [47]. PP possesses excellent resistance to organic solvents,

degreasing agents and electrolytic attack. It has a lower impact strength, but it's working temperatures and tensile strength are superior to low or high density polyethylene. It is light in weight, resistant to staining, and has a low moisture absorption rate. This is a tough, heat-resistant, semi-rigid material, ideal for the transfer of hot liquids or gases. It is recommended for vacuum systems and where higher heats and pressures are encountered. It has excellent resistance to acids and alkalies, but poor aromatic, aliphatic and chlorinated solvent resistance [48].

In general, α-olefins such as PP can not be polymerized by either radical or ionic catalysts. While atactic PP can be produced by use of a Lewis acid or organometallic compound, the product is a branched, rubbery polymer (Tg = -20^{0}C) at ambient temperature with no important commercial applications. In the 1950s, Nata showed that Ziegler-type catalyst could be used to produce stereoregular PP with high crystallinity; however, in contrast to the polymerization of high-density-polyethylene (HDPE), the coordination polymerization of α-olefins is slower and more critically dependent on the nature of the catalyst. The commercial plastic, first introduced in 1957, is highly isotactic (i.e. *i*-PP). High-molecular-weight (150,000 to 1,500,000) *i*-PP can be obtained by using a heterogeneous catalyst of a violet crystalline modified titanium (III) chloride with a cocatalyst or activator, usually an organoaluminum compound such as diethylaluminum chloride. Catalyst are slurried in a hydrocarbon mixture, which helps to facilitate heat transfer in batch or continious reactors operating at temperatures of 50^{0}C to 80^{0}C and pressure of 5 to 25 atm. Hydrogen, which acts as a chain-transfer agent, may be used to moderate molecular weight. Syndiotactic PP(*s*-PP) can be produced by using homogeneous Ziegler-Natta catalyst at lower temperatures. Compared to its isotactic counterpart, *s*-PP has a slightly lower T_m and is more susceptible to solvent attack [49].

$$\left[\!-CH_2\!-\!CH\!-\!\right]_n$$
$$|$$
$$CH_3$$
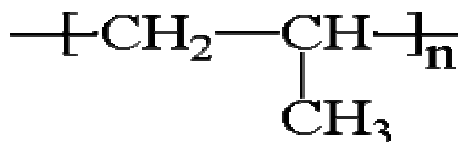
Figure 1.12 Structure of Polypropylene

In general homopolymers (i.e. with only one type of monomer) can be used for housing, housewares, packaging, cassette holders and fibers, monofilaments and film tapes; copolymers (i.e. different monomers are involved) are prefered for all applications exposed to cold and they are widely used for pipes, containers, boat hulls, seat shells and automotive parts e.g. battery cases and bumpers.

Polypropylene can be manufactured to a high degree of purity to be used for the semiconductor industry. Its resistance to bacterial growth makes it suitable to be used in medical equipment. Polypropylene is used in most of our nonwoven fabrics such as rope used in a variety of industries, including fishing and agriculture. PP can be used for flexible packaging applications (e.g. yogurt containers, syrup bottles, straws, etc.), construction sector (e.g. drainage pipes, pumps, etc.), automotive sector, etc [50].

1.12 Aim of the Study

Montmorillonite/polymer nanocomposites have gained considerable interest in recent years. The homogeneous dispersion of montmorillonite clays in polymer matrixes could lead to enhancement in thermal stability, mechanical properties, gas permeability and ionic conductivities. The aims of this study are to synthesize PPy/OMMT nanocomposites chemically, to investigate the thermal, mechanical, electrical conductivity, morphological features and the dispersion of nanoparticles in the polymer matrix then to compare the properties of these nanocomposites with that of pure PPy.

Since PPy/MMT composites are infusible and inprocessable, composites of PPy with an elastomer (PP) were prepared for the purpose of obtaining conductive materials having improved processability and better mechanical properties.

CHAPTER 2

EXPERIMENTAL

2.1 Materials

The materials used have been: (i) Pyrrole (monomer), which was purchased from Sigma Aldrich Chemie GmbH.(Table 2.1), distilled under vacuum and stored in a refrigerator before use. (ii) The filler used is montmorillonite, a sodium calcium aluminum magnesium silicate hydroxide, produced by Sigma Aldrich Chemie GmbH.(Table 2.2) (iii) Anhydrous iron(III) chloride ($FeCl_3$), produced by Sigma Aldrich Chemie GmbH, was used as catalyst. (iv) Ammonium persulfate (APS) (98%, Merck) and dodecylbenzene sulfonic acid (DBSA) were functioned as oxidant and acid dopant (v) Dodecylamine was used as an intercalating agent produced by Sigma Aldrich Chemie GmbH (vi) Methanol used in the washing process was obtained from Aklar Kimya. (vii) HCl was purchased from Sigma Aldrich Chemie GmbH.

Table 2.1 Properties of Pyrrole

Molecular formula	C_4H_5N
Molar mass	67.09 g/mol
Density	0.967 g/ml
Melting Point	-23 ^{0}C
Boiling Point	129-131 ^{0}C

Table 2.2 Properties of Montmorillonite

Molecular formula	(Na Ca) (Al Mg)$_6$ (Si$_4$O$_{10}$)$_3$ (OH)$_6$ nH$_2$O
Molar mass	540.6 g/mol
Density	2.35 g /cm^3
Color	White, yellow

Table 2.3 Properties of Polypropylene

Molecular formula	(C$_3$H$_6$)$_n$
Molecular weight of repeat unit	42.08 g/mol
Amorphous density	0.85 g/cm^3
Crystalline density	0.95 g/cm^3
Glass transition temperature	0 ^{0}C
Melting temperature	173 ^{0}C

2.2 Synthesis of PPy/MMT Nanocomposites

2.2.1 Preparation of Organophilic Clay

Na$^+$-montmorillonite (20 g) was dispersed in 500 mL of water (60^{0}C) by using a mechanical stirrer. To obtain alkylammonium salt, dodecylamine (8.51 g) and concentrated hydrochloric acid (4.6 mL) were dissolved in 100 mL of water. Homoionic CH$_3$(CH$_2$)$_{11}$NH$_3^+$ forms were prepared by ion exchange with alkylammonium chloride salt in water. This was poured into the montmorillonite-

water solution under vigorous stirring for 1 hour. The mixed solution was stirred for 24 hours at 60^0C. The reaction product was filtered at room temperature and then repeatedly washed with distilled water until no AgCl precipitate was observed by a 0.1 N AgNO$_3$ solution, and then dried in an oven under vacuum at 60^0C. This product was termed as C12-MMT.

2.2.2 *In situ* Intercalative Polymerization of PPy with APS

As a representative step to prepare the Polypyrrole/OMMT nanocomposite materials; first, organophilic-MMT was introduced into 400 mL distilled water under magnetic stirring overnight at room temperature. Pyrrole monomers (10 g, 0.3 mol) and DBSA (24.3 g, 0.15 mol) were subsequently added to the previous solution, which was stirred for another 24 h at 5°C. Upon addition of ammonium persulfate (6.8 g, 0.06 mol) in 100 mL distilled water, the solution was stirred for 40 h at 5°C and then terminated by pouring large amount of methanol into the solution. PPy/OMMT nanocomposite materials were then precipitated from the mixing solution as a black powder, followed by filtering and sequentially washing with distilled water, methanol, and acetone several times. The as-synthesized DBSA-doped nanocomposite precipitates were then obtained by drying under vacuum at 30°C for 12 h.

2.2.3 *In situ* Oxidative Polymerization of PPy with FeCl$_3$

An oxidant, 0.1 mol (16.2 g) anhydrous FeCl$_3$ dissolved in 100 mL of distilled water was mixed with 0.01 mol of surfactant (DBSA) dissolved in 100 mL distilled water in reaction vessel and stirred for 15 min. The 0.15 mol pyrrole (10.4 mL) dispersed in 50 mL of water was inserted dropwise into the stirred mixture of an oxidant and surfactant. The polymerization was carried out for 4 hours at room temperature at moderate stirring. The precipitated PPy was filtered off and washed with distilled water. The black PPy powder was dried in a vacuum oven at 60- 80^0C for 8 hours.

2.3 Preparation of PPy/PP Composites

2.3.1 Preparation of mixed and moulded composites

PP/PPy composites were prepared by mixing virgin PP with chemically synthesized PPy at 60 rpm for 30 minutes using Brabender Plasti-Corder. Obtained composites were compressed in a mould for 5 minutes at 210 ^{0}C and then these moulds were fast cooled. Percentage of PPy in the composites were 2, 5, 10, and 20 with respect to total weight.

2.3.2 Injection Molding

The specimens for mechanical characterization were prepared by injection molding using a laboratory scale injection molding machine (Microinjector, Daca Instruments). During molding; barrel temperature (210 ^{0}C), mold temperature (0 ^{0}C), injection pressure (16 bars) and cycle time (3 min) were identical for the preparation of each sample.

2.4 Characterization

2.4.1 Fourier Transform Infrared Spectrometer (FTIR)

FTIR spectra of the samples were recorded on a Bruker IFS 66/S FTIR spectrometer in order to detect the functional groups.

2.4.2 Thermal Gravimetric Analysis (TGA)

The thermal gravimetric analysis were performed by a Perkin Elmer Pyris1 Thermal Gravimetric Analyzer. Samples were examined at a heating rate of 10 ^{0}C/min. under N$_2$ atmosphere.

2.4.3 Conductivity Measurements

Conductivity measurements were performed by four probe technique at room temperature. Two of the probes were used to source current and the other two probes are used to measure voltage (Figure 2.1). In four probe technique, four equally spaced osmium tips were placed onto a head. The head was lowered to the sample until the four probes touch with the sample. The current source supplied the steady current through the outermost probes and the voltage drop across the inner two probes was measured.
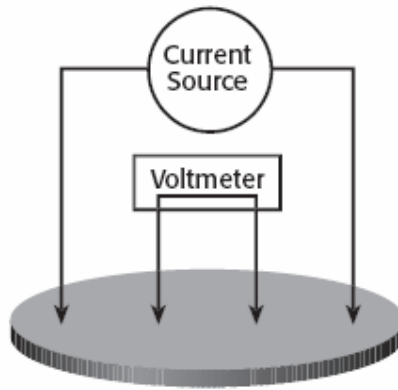
Figure 2.1 Four Probe Technique

Conductivity was given by the equation $\sigma = \ln2.I/\pi.d.V$

Where σ is the conductivity, I is the current passes through the outer probes, V voltage drop across the inner probes and d is the sample thickness. Using four probes eliminates measurement errors due to the probe resistance, the spreading resistance under each probe, and the contact resistance between each metal probe and the specimen material. In order to determine conductivities, current voltage measurements were done using FPP 0602 Electrometer.

2.4.4 Tensile Tests

Tensile tests were performed for each composition according to ASTM D638 (Standard Test Method for Tensile Properties of Plastics), by using a Lloyd LR 30K Universal Testing machine. The shape and dimensions of the specimens are given in Figure 2.2 and Table 2.3.
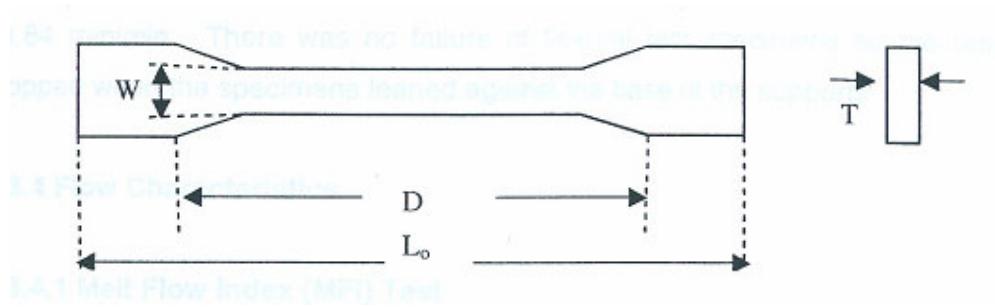
Figure 2.2 ASTM Tensile Test Specimen

Table 2.4 Dimensions of tensile test specimen

Symbol	Specimen Dimensions (mm)
W, Width of narrow section	7.4
D, Distance between grips	50
L_0, Total length of specimen	110
T, Thickness of specimen	2.05

In discussing tensile properties it is of importance to be familiar with some terms.

Stress: Stress is defined as the force per unit area perpendicular or normal to a force.

Stress $(\sigma) = F/A_0$

Strain: Strain is defined as $\varepsilon = \Delta D / D$

where; D = original gauge length and ΔD = the change in gauge length due to deformation

Tensile Strength: It is calculated by dividing the maximum load in Newtons by the original cross-sectional area of the specimen. The result is expressed in terms of mega Pascal.

Tensile Strength = Force (Load) (N) /Cross Section Area (mm^2)

Young's Modulus: It is also called the tensile or elastic modulus. Young's Modulus can be calculated from the initial straight line portion of a stress-strain curve; tensile modulus is the slope of this line. The result is expressed in MPa unit.
Young's Modulus = Difference in Stress / Difference in Corresponding Strain

Tensile Strength at Break: When maximum stress occurs at break, it is designated as Tensile Strength at Break. The result also is expressed in MPa unit.
Tensile Strength at Break: Load Recorded at Break / Cross Section Area (mm^2)

Tensile Strain at Break: It is the main strain measured at the breaking point.

The crosshead speed used in measurements was 5.0 cm/min. The test was performed by pulling the specimens from both grips until it fails. Stress versus strain diagrams were obtained from the mechanical testing device and tensile strength, tensile modulus, tensile strain at break and values were determined by using these graphs.

2.4.5 X-Ray Diffraction (XRD) Analysis

The composites were analyzed by using a Rigaku Miniflex X-Ray diffractometer. Cu-K anode radiation, generated at a generator tension of 30 kV and and a generator current of 15 mA was used as the X-Ray source. The diffraction patterns

were collected at a diffraction angle 2θ from 4^0 to 35^0 at a scanning rate and step size of 1^0/min and 0.05^0, respectively.

2.4.6 Scanning Electron Microscopy (SEM)

JEOL JSM-6400 low voltage scanning electron microscope was used for morphological studies of composites. Before SEM photographs were taken, the fractured surfaces of PP/PPy composites were coated with a thin layer of gold in order to obtain a conductive surface. Specimens were viewed using the secondary electron image with an accelerating potential of 20 kV; at the magnification used. The main purpose was to observe the way by which the OMMT dispersed in the PPy matrix and the fracture behaviour of the PPy/PP composites.

CHAPTER 3

RESULTS AND DISCUSSION

3.1 PPy/OMMT Nanocomposites

3.1.1 Synthesis of PPy/OMMT Nanocomposites

In situ intercalative polymerization with APS: This process involves mixing of the clay mineral with the required monomer. The monomer then intercalates within the interlayer and promotes delamination. Upon addition of APS, polymerization begin to occur and get yield polymer matrices. Using this method, the PPy/clay nanocomposites whose clay content changing 1% to 15% were obtained

In situ oxidative polymerization with FeCl$_3$: The required monomer and DBSA were put the reaction media then the addition of FeCl$_3$ immediately changed the mixtures from colourless to black. This was indicative of a charge transfer reaction between the Fe^{+3} centers and lone pairs on the N atoms in Py leading to the formation of [Py$^+$]. The obtained PPy had a greater conductivity value than PPy obtained by using APS (about 100 times). Because of that reason, PPy which was synthesized by FeCl$_3$ was used inorder to investigate the behaviour of PP/PPy composites and the weight content changing %2 to 20% composites were prepared.

3.1.2 FTIR Spectra of PPy/Org.-MMT Composites

The characteristic FTIR spectra of the organophilic MMT, MMT, pristine PPy, and PPy/OMMT nanocomposite materials were illustrated in Figure 3.1, 3.2, 3.3, 3.4. According to Figure 3.1, the characteristic absorption bands of MMT are 1073 cm^{-1}

for Si-O-Si stretching, 1615 cm^{-1} for H-O-H bending, 799 cm^{-1} for Si-O deformation, 524 cm^{-1} for Al-O, 463 cm^{-1} for Mg-O. For OMMT, the characteristic absorption bands include CH_2 asymmetric stretching at 2928 cm^{-1}, CH_2 symmetric stretching at 2853 cm^{-1}, CH_2 plane scissoring at 1471 cm^{-1} and these bands came from dodecylamine which is intercalating agent. In addition, absorption bands which are the characteristic bands of MMT related to silicate are also found in Figure3.1, such as 1618 cm^{-1} for H-O-H bending, 1061 cm^{-1} for Si-O-Si stretching, 801 cm^{-1} for Si-O deformation 522 cm^{-1} (Al-O), and 466 cm^{-1} (Mg-O). This result shows that the intercalation of alkylammonium cations between the silicate layers.
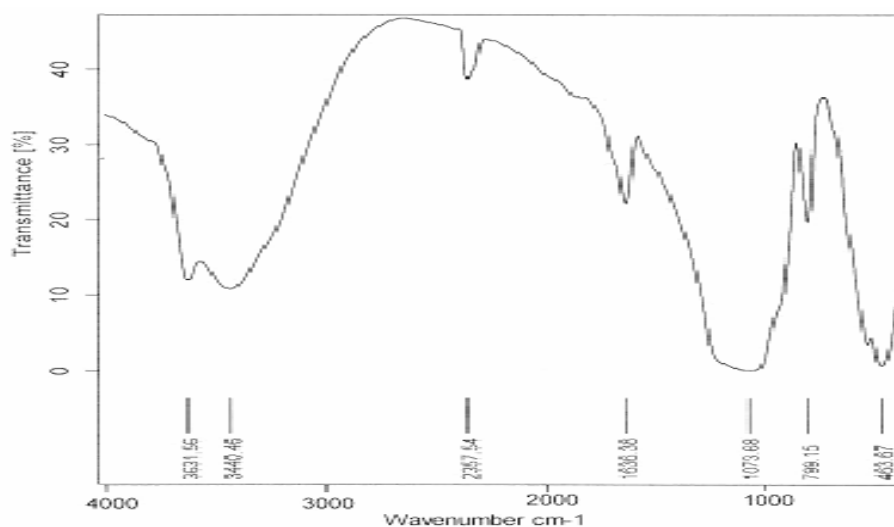
Figure 3.1 FTIR spectrum of MMT
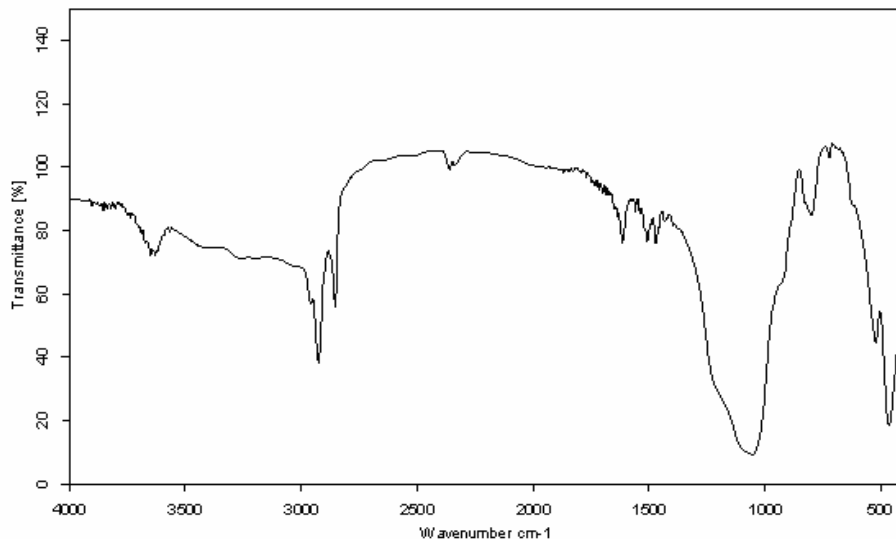
Figure 3.2 FTIR spectrum of OMMT

The representative vibration bands of PPy were at 1539 cm^{-1} (2,5-substituted pyrrole), 1037 cm^{-1} (C-H vibration of 2,5-substituted pyrrole), and 902 and 726 cm^{-1} (C-H deformation of 2,5-substituted pyrrole) and the peak at 1168 cm^{-1} is from S=O stretching vibration of sulfonic acid (Figure 3.3).
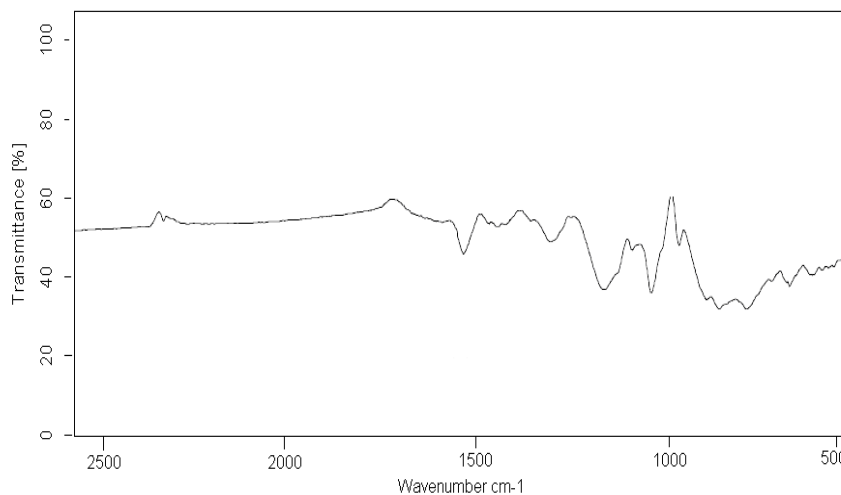
Figure 3.3 FTIR spectrum of PPy

42

Peaks coming from both OMMT and PPy were observed in the FTIR spectra of PPy/OMMT composites (Figure 3.4). The appearance of peaks 1539, 1037, 902 and 726 cm^{-1} in the composite and the PPy homopolymer readily endorsed the incorporation of PPy in the composite backbone. Also, the composite's FTIR spectrum clearly shows the presence of characteristic peaks of OMMT at 2923, 2852, 1459, 580 and 426 cm^{-1}. Thus, FTIR data confirmed the incorporation of either moieties in the structure of the composite. Also, as the loading of clay content in the composites was increased, the characteristic peaks of clay bands became sharper in the FTIR spectra of PPy/clay materials.
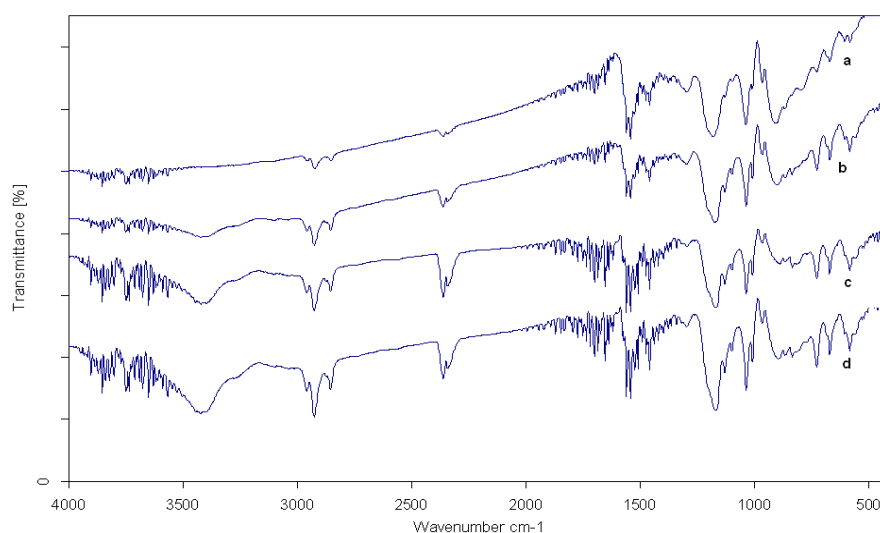
Figure 3.4 FTIR spectrum of PPy/clay nanocomposites; a) PPy/1%OMMT, b) PPy/5%OMMT, c) PPy/10%OMMT, d) PPy/15%OMMT nanocomposites.

3.1.3 X-Ray Diffraction (XRD) Analysis

A typical synthesis of polymer–clay nanocomposites involves organic modification of clay with the alkylammonium cation and intercalation of a suitable monomer followed by *in situ* polymerization. The role of the alkylammonium cation is to improve penetration of the organophilic monomers into the interlayer space and the

role of the monomer is to promote dispersion of the clay particles. The increased basal spacing arises from the expansion of the interlayer space to accommodate the polymer; as a result, the intercalation process of polymers can be distinguished from the difference in basal spacing [51]. By monitoring the position The basal spacing (d001) from XRD measurement is calculated at peak positions according to Bragg's law:

$$d = \lambda /(2 \sin \theta), \qquad \text{where } \theta \text{ is the diffraction angle.}$$

In the case of exfoliated nanocomposites, the extensive layer separation associated with the delamination of the original silicate layers in the polymer matrix results in the eventual disappearance of any coherent X-ray diffraction from the distributed silicate layers. On the other hand, for intercalated nanocomposites, the finite layer expansion associated with the polymer intercalation results in the appearance of a new basal reflection corresponding to the larger gallery height [33].

Interlayer spacing increased with increasing primary aliphatic-amine length. In general, greater spacing would be advantageous in the intercalation of a polymer. It would also lead to easy dissociation of MMT, which would result in hybrids with better dispersion of MMT. Figure 3.5 shows the XRD patterns of MMT and OMMT when 2θ varies from 4^0 to 12^0. The XRD pattern of pure MMT shows a characteristic peak (d001=9,71 Å) at 9.10^0 of 2θ. However, the basal spacing of OMMT is 10.97Å (Table 3.1). The (001) peak is shifted toward a lower angle and the space between the layers become larger. This clearly indicates the intercalation of alkylammonium cations between the silicate layers.

Table 3.1 d spacing of the MMT and OMMT with the corresponding diffraction angle.

MMT		OMMT	
d-spacing (Å)	$2\theta^0$	d-spacing (Å)	$2\theta^0$
9.71	9.10	10.97	8.05

The wide angle X-ray diffraction (XRD) pattern of OMMT clay showed a peak $2\theta^0=8.05^0$ (d-spacing = 10.97 Å) in the direction of d(001) indicative of the expected interlayer distance between two silicate layers. This spacing was sufficient for intercalation of PPy in the clay which was endorsed by the XRD pattern of PPy/OMMT composite. A sharp XRD peak appeared at 2θ of 9.05^0 for the OMMT as shown in Figure 3.5, indicating that the interlayer distance of OMMT was 10.97 Å, based on the Bragg equation ($n\lambda=2d\sin\theta$).
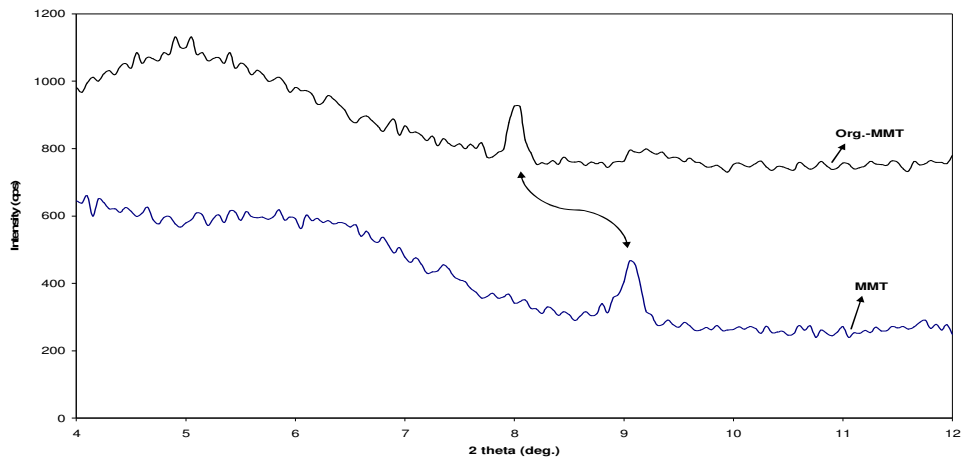
Figure 3.5 XRD pattern of MMT and OMMT

In the case of 1 % PPy/clay composite, a broad WXRD peak appeared at 2θ of 5.30^0 (Table 3.3), indicating the intergallery distance had been increased to 16.65 Å

(Table 3.2) by intercalation of PPy material between the clay layers during nanocomposite synthesis. Also, 1% PPy/OMMT nanocomposite has peaks at 10.15^0, 17.60^0, 24.50^0 (Table 3.3) indicating that the dispersion of clay platelets into PPy matrix led to an effective increase in the polymeric crystallinity resulted from the heterogeneous nucleating effect of layered silicate existing in polymer matrix. According to Table 3.3 and Table 3.2, as the loading of clay was increased in the PPy/OMMT composite system, diffraction peaks were shifted toward lower angle and the basal spacing values getting larger slightly.

Table 3.2 d-spacing values of OMMT and PPy/OMMT nanocomposites.

	OMMT	1% PPy/OMMT	5% PPy/OMMT	10% PPy/OMMT	15% PPy/OMMT
d-spacing (Å)	10.97	16.65	16.97	17.14	17.31
	4.92	8.70	8.84	8.88	8.92
	4.42	5.03	5.08	5.09	5.11
	3.29	3.63	3.65	3.66	3.67

Table 3.3 2θ values of OMMT and PPy/OMMT nanocomposites

	OMMT	1% PPy/OMMT	5% PPy/OMMT	10% PPy/OMMT	15% PPy/OMMT
$2\theta^0$	8.05	5.30	5.20	5.15	5.10
	18.25	10.15	10.00	9.95	9.90
	20.30	17.60	17.45	17.40	17.35
	27.05	24.50	24.35	24.30	24.20
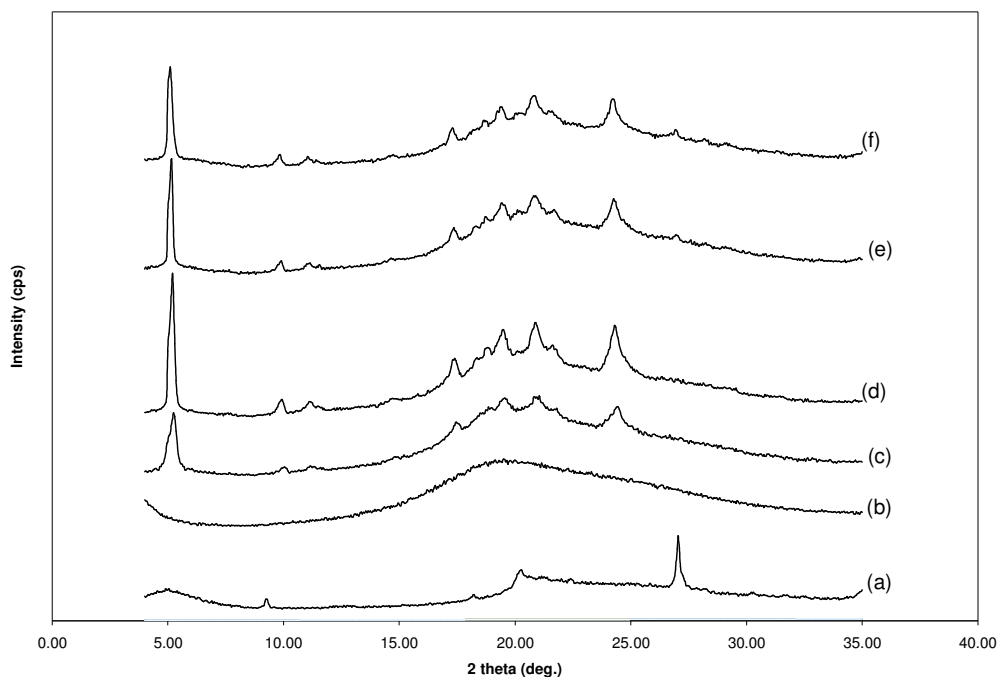
Figure 3.6 XRD pattern of PPy/OMMT composite prepared by *in situ* intercalative polymerization; a) OMMT, b) PPy, c) PPy/1%OMMT, d) PPy/5%OMMT, e) PPy/10%OMMT, f) PPy/15%OMMT

3.1.4 Electrical Conductivity Measurements

Conductivity of composites were measured at room temperature using four probe technique. The conductivity values for various PPy/OMMT nanocomposites were in the order of 10^{-3} S/cm are presented in Table 3.4. Electrical conductivity of composite materials in the form of a powder-pressed pellet was found slightly smaller than that of PPy homopolymer, as shown in Table 3.4. This was expected because composites have more insulating states than PPy [52] and the clay layers are regarded to interrupt the effective doping and weaken the interchain interaction of polymer main chains resulting in low conductivity of the nanocomposite systems [39]. Also, clay component was not electronically conductive and the incorporation

of clay into PPy matrix contributed a smaller molecular weight, leading to a lower electrical conductivity [46].

Table 3.4 Conductivity values of PPy/OMMT nanocomposites

	Conductivity (Scm^{-1})
PPy	$2,3.10^{-2}$
1 % OMMT/PPy	$6,8.10^{-3}$
5 % OMMT/PPy	$2,8.10^{-3}$
10 % OMMT/PPy	$1,0.10^{-3}$
15 % OMMT/PPy	$8,7.10^{-4}$

3.1.5 Thermal Properties of PPy/Organo-MMT Composites

3.1.5.1 Thermal Gravimetric Analysis (TGA)

The thermal stabilities of PPy and their nanocomposites in N_2 were studied by TGA. According to the published reports on polymer-clay nanocomposite materials, the unparalleled ability of smectite clays was found to boost the thermal stability of polymers. Figure 3.7 shows wieght loss versus temperature date for MMT, and OMMT; and Figure 3.8 represent weight loss versus temperature data for PPy, and PPy/OMMT nanocomposites.

According to TGA thermographs, for MMT (Figure 3.7 a), a weight loss (~10%) between 50^0C and 950^0C seems because of water elimination and the structural water that is the bonded hydroxyl groups. However, organically modified MMT (Figure 3.7 b) loses about 36% of their total weight between the same temperature range. There are four major stages of weight loss for OMMT. The first weight loss between 50^0C and 100^0C (~1%) is a release of free water. The second and third

stages in the temperature range 250-550^{0}C are associated with the decomposition of organic substances present in OMMT and loss in temperature 550-750^{0}C, the bonded hydroxyl groups start to decompose.
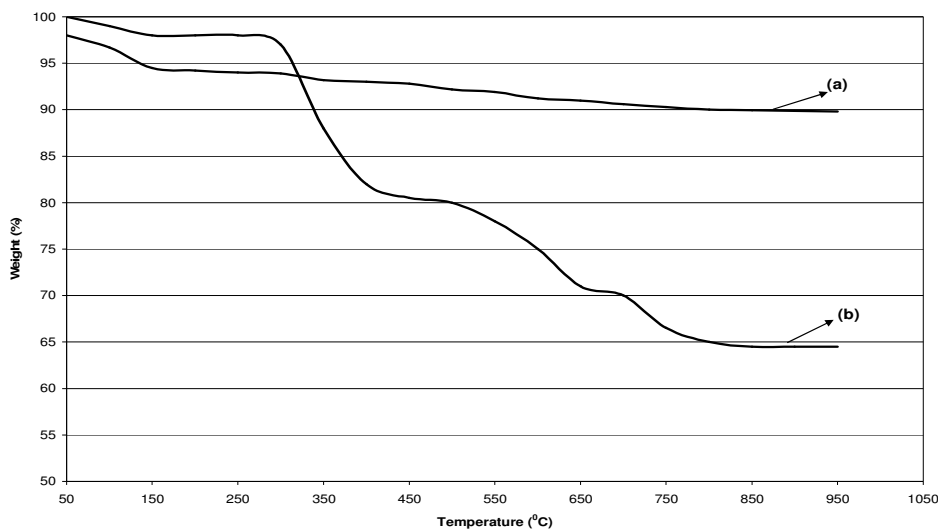
Figure 3.7 TGA curve of a) MMT and b) OMMT

As for PPy (Figure 3.8 a), a small weight loss (~0.5%) up to around 100^{0}C is presumably due to the elimination of water and other volatiles. The weight loss occuring between 200 and 450^{0}C (~22%) is approximately the weight fraction of DBSA; therefore it is attributed mainly to the dopant loss. It has been suggested that the lower temperature decomposition (250-300^{0}C) is that of the excess DBSA, and the higher one (300-450^{0}C) is that of the bound DBSA. Above 450^{0}C, the polymer itself decomposes and at 800^{0}C all polymer material is decomposed. The TGA thermogram (Figure 3.8 (curves b,c,d,e)) of the PPy/OMMT clay nanocomposites showed several stage of weight loss starting at 270^{0}C and ending at 900^{0}C, which might correspond to the degradation of the intercalating agent followed by the structural decomposition of the polymers. The first weight loss below 100^{0}C (~2-3%) is a result of the release of free water. The second stages in the temperature range 270^{0}C-800^{0}C are associated with the dopant loss the decomposition of polymer and the decomposition of organic substances present in the organo clay.

49

The lower molecular weight organics are released firts at the lower temperature, followed by the higher molecular weight organics. In the last stage of weight loss in the the temperature range 600^0C-780^0C the structural water that is the bonded hydroxyl groups start to decompose and are being released. After ~ 700°C, the curve all became flat and mainly the inorganic residue (i.e., Al_2O_3, MgO, SiO_2) remained. From the amounts of the residue at 700°C, the inorganic contents in the original PPy/clay materials can be obtained, which were significantly higher than the values calculated from the feed composition. The calculated inorganic contents tend to be lower than those determined from TGA probably because of low yield of PPy prepared from pyrrole monomers in PPy/OMMT materials

The weight loss observed for PPy about 800 ^0C was 100%. However, The weight remaining of PPy/clay nanocomposites whose clay contents are 1%, 5%, 10 % and 15% were 8.4%, 16.8%, 29.3% and 34.4% respectively at the same temperature. Hence, the thermal stability of nanocomposites are beter than pure PPy and also the thermal stability of nanocomposites increases with increasing OMMT content in the PPy/OMMT system.
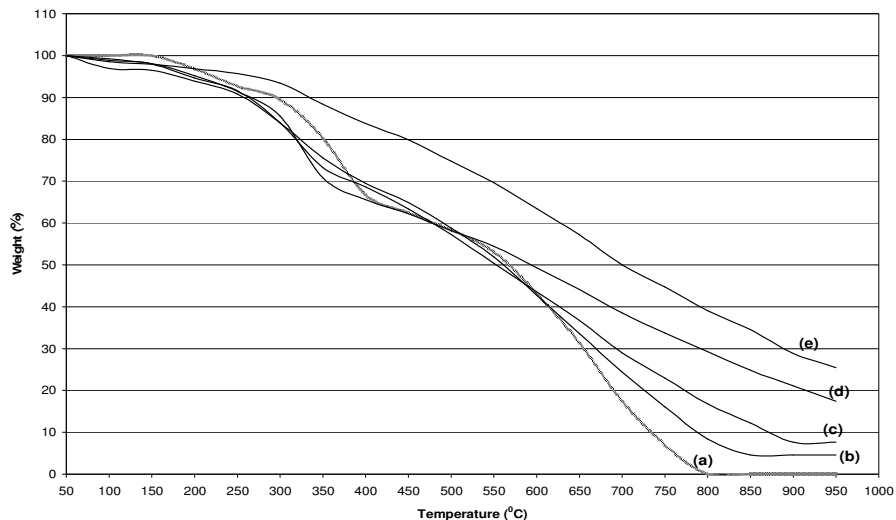
Figure 3.8 TGA curve of PPy and PPy/OMMT nanocomposites; a) PPy, b) PPy/1%OMMT, c) PPy/5%OMMT, d) PPy/10%OMMT, e) PPy/15%OMMT

3.1.6 Scanning Electron Microscopy (SEM) Analysis

In order to investigate the effect the morphological properties of PPy/OMMT composites scanning electron microscopy analysis was performed to all samples produced.

Scanning electron micrographs of MMT, OMMT, PPy and PPy/OMMT composites are presented in Figure 3.9 and Figure 3.10. SEM micrographs show that MMT (Figure 3.9 a) has flaky particles arranged into the form of spheres with irregular size. OMMT particles are similar but have smaller size spheres and partial rearrangement of MMT spheres by organic modifier (Figure 3.9 b).
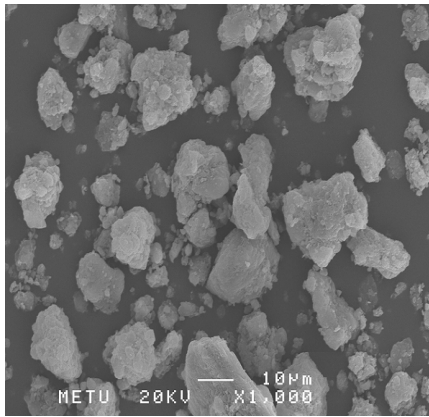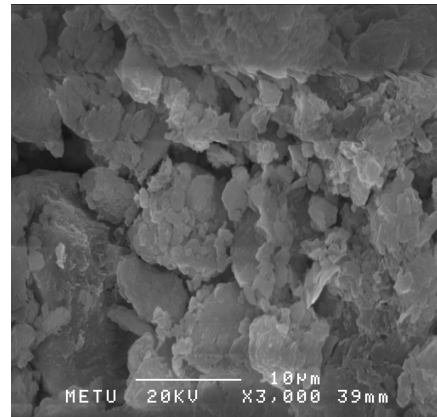
(a) MMT   (b) OMMT

Figure 3.9 SEM micrographs of OMMT and MMT

SEM micrographs of PPy exhibits submicrometer-size, bright globular particles. Also, PPy (Figure 3.10 a) showed loose-packing morphological image, reflecting a low crystallinity of pristine electronically conductive PPy matrix. According to

SEM micrographs the morphology of the PPy/clay nanocomposites differ slightly from that of the clay. Because the particles undergo some rearrangement of the original OMMT flakes, so PPy slightly modified the flaky structure of the OMMT nanoparticles. Morover, the surface exhibits some bright inclusions that could be assigned to PPy as judged. The sand-like colour of OMMT particles changed to grey or black, depending on the amount of PPy formed, indicating the covering of OMMT particles with PPy especially this was seen in composites which were PPy/1%OMMT (Figure 3.10 b) and PPy/5%OMMT (Figure 3.10 c). The typical PPy structure is hardly visible. However, the SEM micrograph of PPy/10%OMMT (Figure 3.10 d) and PPy/15%OMMT (Figure 3.10 e) showed wealthy and much larger compact-packing of crystalline domains, corresponding to a polymer matrix with higher crystallinity, which was consistent with the results obtained from the wideangle powder X-ray diffraction pattern studies.
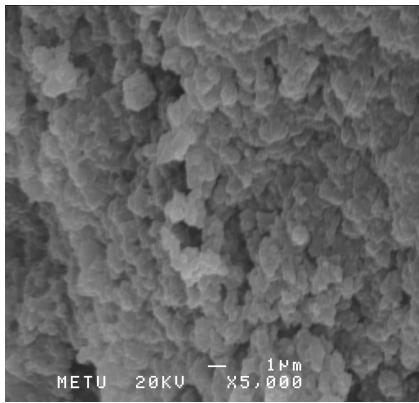
(a) PPy
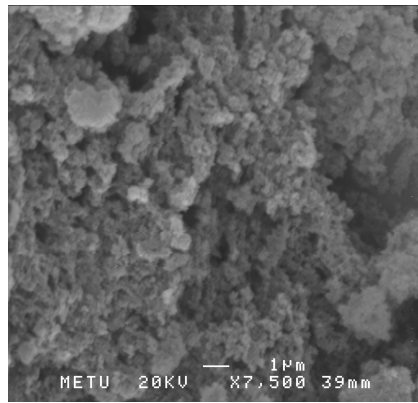
(b) PPy/1%OMMT
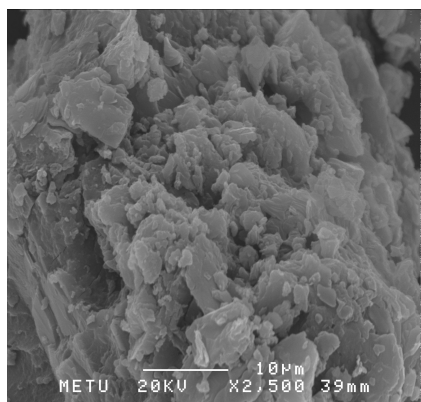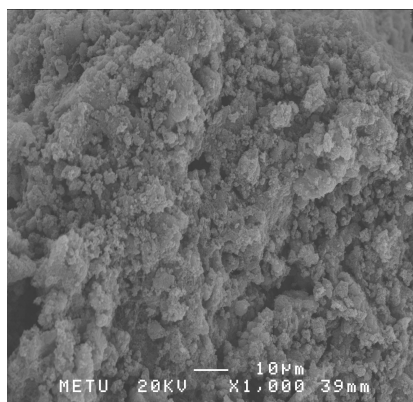
(c) PPy/5%OMMT   (d) PPy/10%OMMT
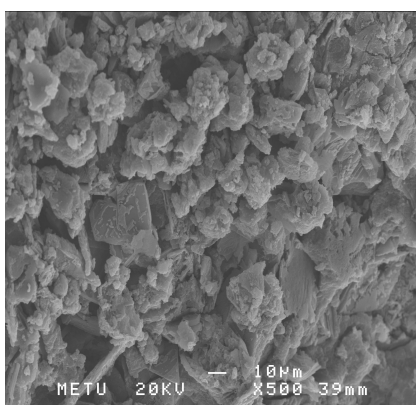
(e) PPy/15%OMMT

Figure 3.10 SEM micrographs of PPy/OMMT

3.2 PP/PPy Composites

3.2.1 Synthesis of PP/PPy Composites

During the last decade there has been widespread interest in conductive polymers both for academic purposes and for potential applications. However, many electroactive polymers suffer from a lack of stability and a poor processability. Up to now, PPy is one of the most useful conducting polymers, since it has high conductivity and good thermal and oxidative stability. But, like most conducting

polymers prepared to date, it is also intractable. In order to improve the processability of polypyrrole, efforts have been made to obtain composites which contain both polypyrrole and nonconductive processible thermoplastic [47]. PP/PPy composites were prepared by mixing PP with chemically synthesized PPy using a Plasticorder Brabender. The amount of conductive polypyrrole was varied between 2 and 20 wt % in composites.

Table 3.5 Data for preparation of PP/PPy composites

PP (g)	PPy (g)	PPy in composite (%wt)
44.1	0.9	2
42.75	2.25	5
40.5	4.5	10
36	9	20

3.2.2 Tensile Properties

In this study, tensile test was performed to investigate the mechanical properties of PP/PPy composites. The loading of PPy with different weight percents into thermoplastic polypropylene matrix produces changes in the mechanical properties of the resulting composites.

The response of a material in a tensile test is well understood by means of stress-strain curve. The effect of different PPy concentration on tensile properties can be seen by stress-strain curves of specimens which are illustrated in Figure 3.11 through Figure 3.14. The response of the materials to applied stress distinguishes them as ductile or brittle. As it is seen from Figure 3.10, the virgin PP is vey ductile

at a test rate of 5 cm/min. The area under the curve is the measure of the energy necessary to break the material. Addition of PPy to the virgin PP, makes it more brittle and decreases the energy required to break it.

All the composites prepared in this study together with the values of the virgin PP are evaluated and the data are presented in Table 3.7. The tensile strain at break (%), tensile strength, and Young's modulus of pure PP were determined as 432.1 %, 26.4 MPa, and 431.9 MPa, respectively. Figure 3.16 demonstrates the effect of PPy content on the tensile strain at break of the composites. Addition of 2 wt % PPy to PP resulted in a dramatic decrease in the tensile strain at break of the material. However, increasing PPy content did not appreciably change the tensile strain at break.

When 2 wt % PPy was added to PP matrix, the tensile strength of PP decreased (Figure 3.17).Because the interaction between PP matrix and PPy was so weak. However, tensile strength increases with increasing PPy content.

Stiffness of the material at the start of a tensile test is expressed by Young's modulus and it is clearly seen that Young's modulus becomes strongly improved when composites are formed (Figure 3.18) As the loading of PPy increases in the composite system, strain will decrease and stress increases, this affects the Young's modulus which increases simultaneously. The increase in Young's modulus is reasonable and expected, because extension of PP matrix is prevented by PPy acting as the reinforcing phase.
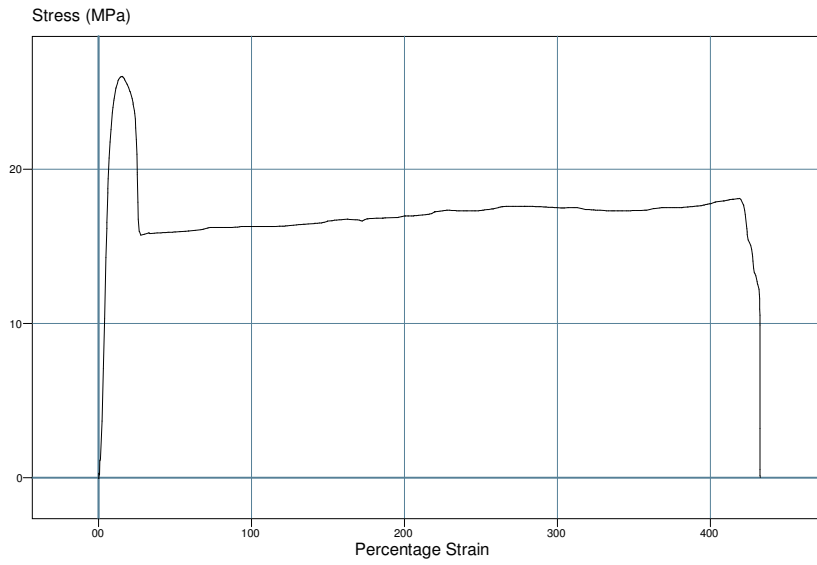
Figure 3.11 Tensile stress-strain (%) curve of polypropylene
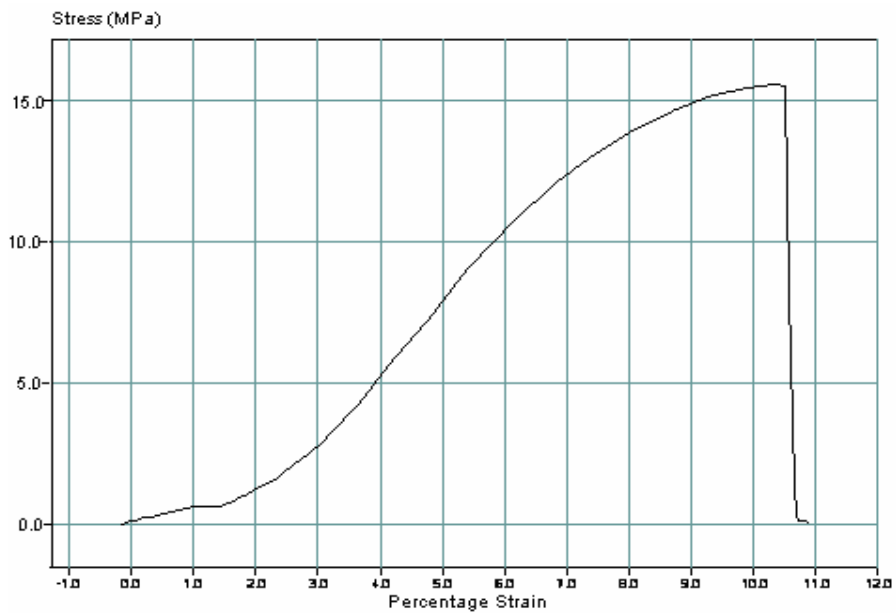
Figure 3.12 Tensile stress-strain (%) curve of 2 % PPy-PP composite
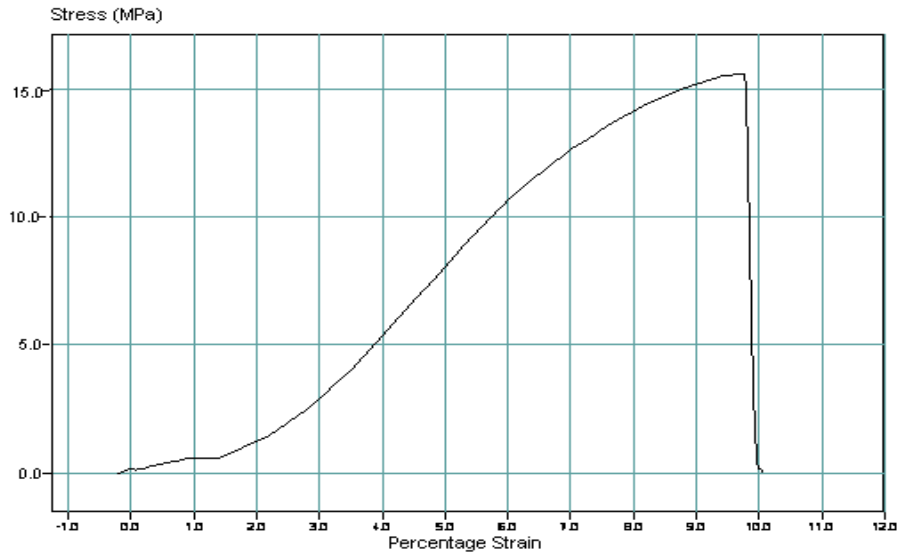
Figure 3.13 Tensile stress-strain (%) curve of 5 % PPy-PP composite
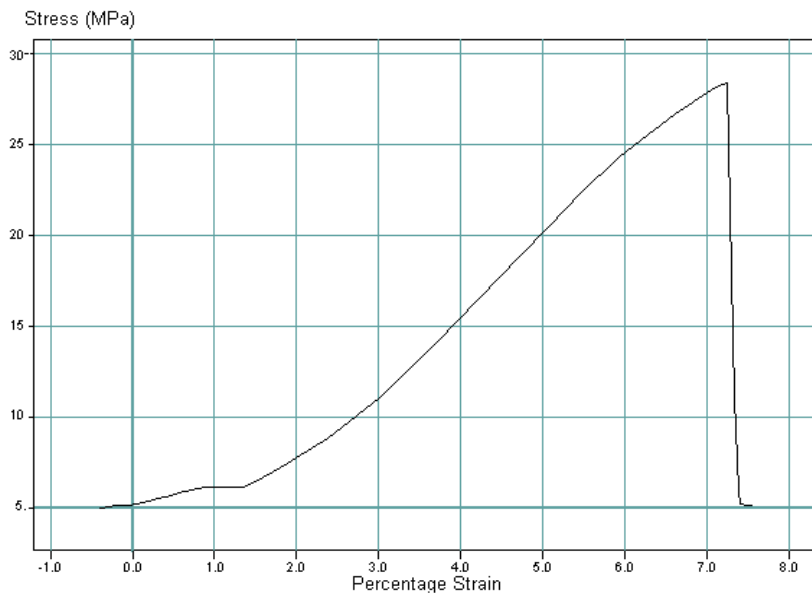
Figure 3.14 Tensile stress-strain (%) curve of 10 % PPy-PP composite
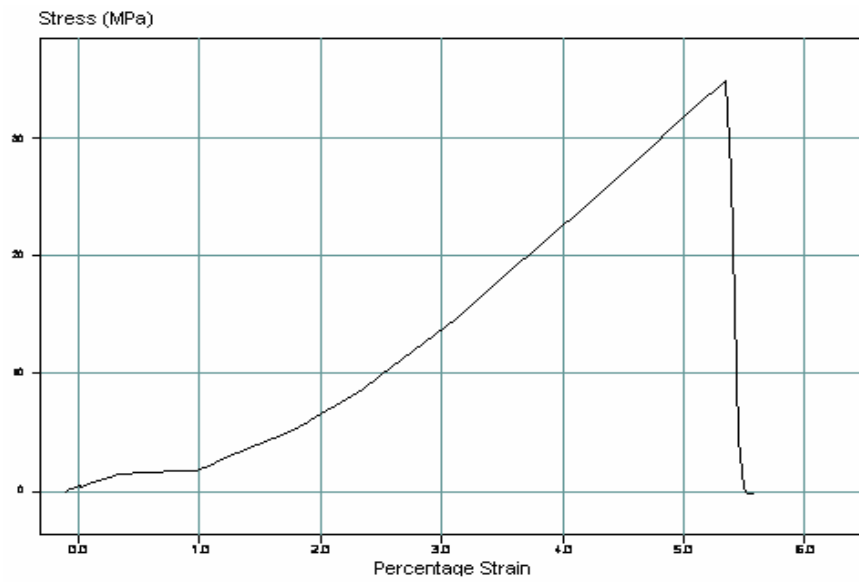
Figure 3.15 Tensile stress-strain (%) curve of 20 % PPy-PP
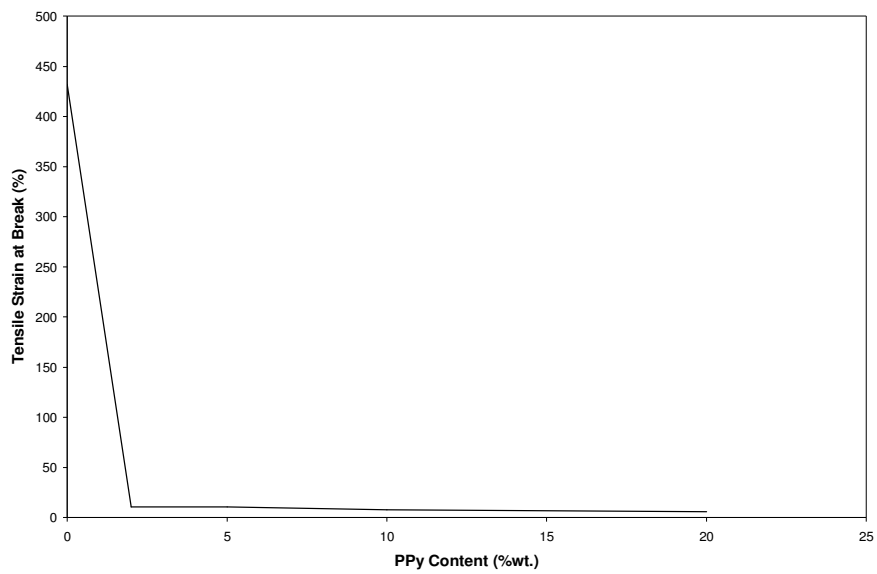
Figure 3.16 Effect of PPy content on the tensile strain at break (%) of composites
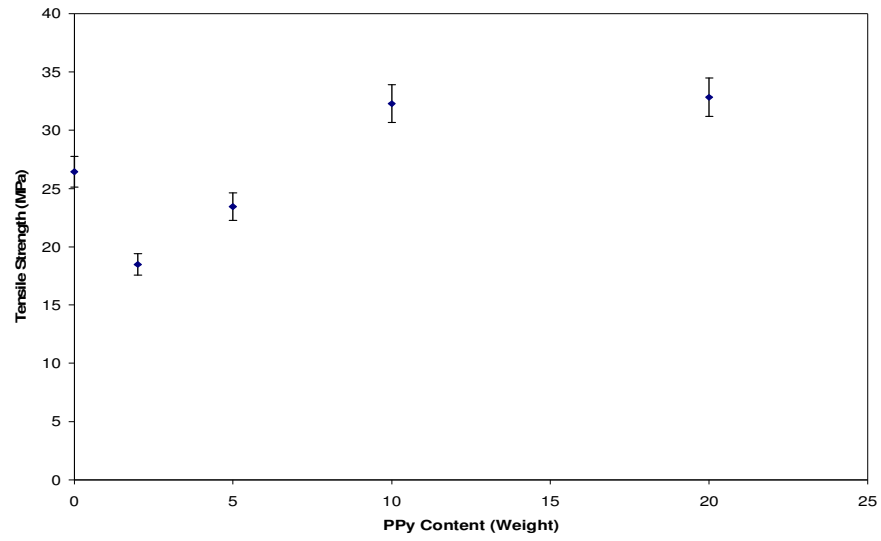
Figure 3.17 Effect of PPy content on the tensile strength of composites
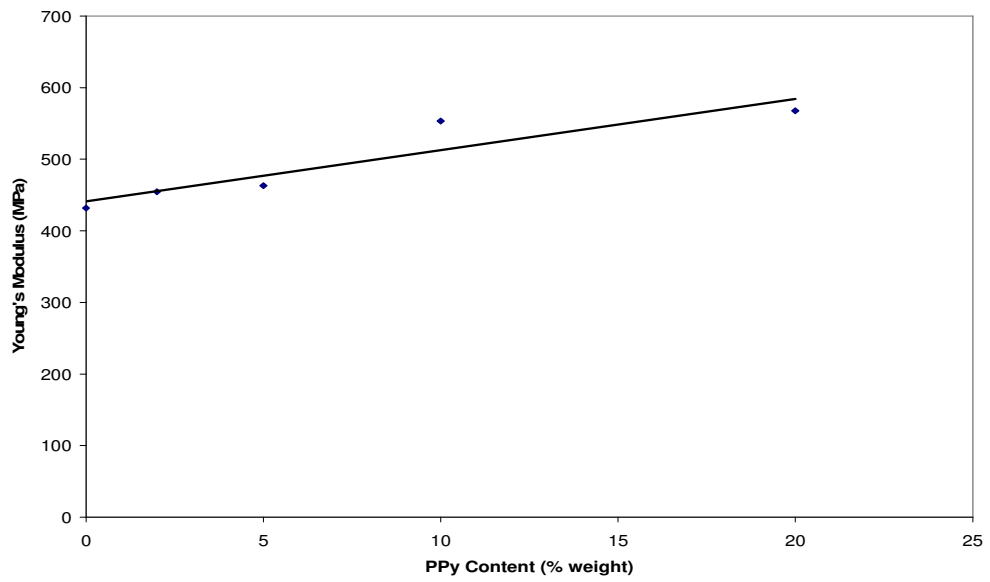
Figure 3.18 Effect of PPy content on the Young's modulus of composites

Table 3.6 Tensile Properties of PP/PPy composites

Wt % ppy	Tensile Strain at Break (%)	Tensile Strength (MPa)	Young's Modulus (MPa)
0	432,12 ± 8,35	26,42±0,55	431,89±9,77
2	10,57 ±0,56	18,49±0.90	454,45±11,78
5	10,53±0,77	23,43±0,15	463,03±12,69
10	7,65±0,34	32,28±1.21	553,33±7,88
20	5,89±0,12	32,82±1.60	567,61±3.86

3.2.3 Electrical Conductivity Measurements

The conductivity of PP, PPy and PP/PPy composites are shown in Table 3.7.Even a very small PPy amount present in composites results in an enourmous enhancement in conductivity by about nine orders of magnitude. Conductivity of prepared composites increases with increasing weight percentage of PPy. This is expected because a conducting polymer is added to an insulating matrix polypropylene.

Table 3.7 Conductivity values of PPy/PP composites

Wt % PPy	Conductivity (Scm^{-1})
0	$1.0.10^{-16}$
2	$3.4.10^{-6}$
5	$5.4.10^{-6}$
10	$1.2.10^{-5}$
20	$4.3.10^{-5}$
100	$3.9.10^{-1}$

It is well known that at low loading of the conductive filler the modest conductivity increase is observed with rising filler content. Sudden conductivity increase and sudden elongation decrease occurs in relatively narrow concentration range around so called percolation threshold. According to Figure 3.19, that point is about 1.8 wt.% for PP/PPy composites.
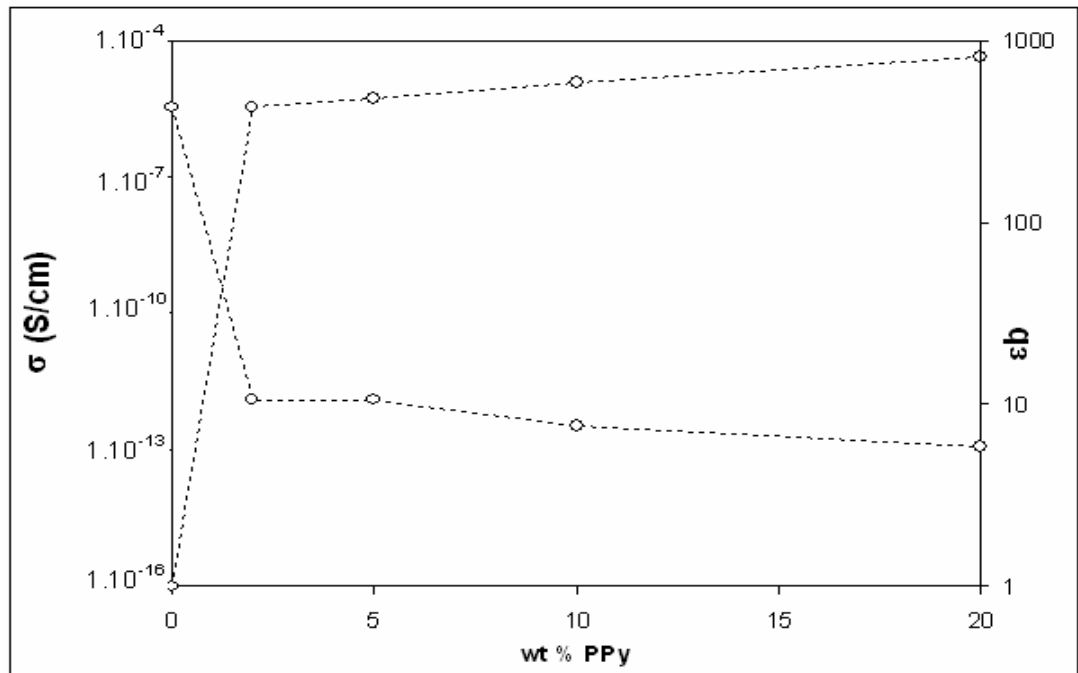
Figure 3.19 Conductivity-Elongation graph of PP/PPy composites

At this concentration a conductive network is formed within the insulating phase and a dramatic increase in conductivity by several order of magnitude is observed.

3.2.4 Scanning Electron Microscope (SEM) Analysis

In Figures 3.19 through 3.22, SEM micrographs of fractured surfaces PP-PPy composites are shown at magnifications of x1000. PP/2%PPy is shown at

magnification x1000 and x5000 respectively. It is seen from Figure 3.20 and Figure 3.21 that 2 % and 5 % PPy/PP composites have smooth surfaces and a few crack propagation lines are observed. Due to the rough surface of the filler, the amount of bound PP increased. As the PPy loading increases in composite system to 10% and 20% (Figure 3.22 and Figure 3.23 respectively), PPy adhered to PP matrix and during tensile test the filler driven out of PP matrix while PP matrix oriented along the draw direction. As the filler loading increases, the amount of polymer needed for complete coating increase. Hence the distance between the filler particles becomes shorter which increase the stress exerted on filler particles resulting in fracture at low stress. Therefore the elongation at break decreased. Also, as the loading of PPy in the composites increase, the brighter the surface of the composites. So, it shows the composites became more conductive [37].

For more precise analysis of the morphology, a more powerful technique like transmission electron microscopy (TEM) analysis should be performed.
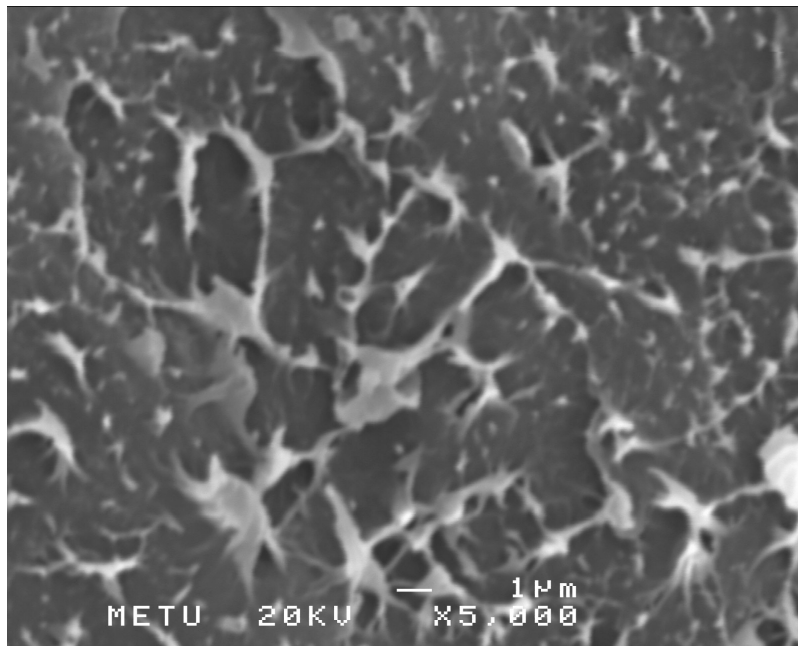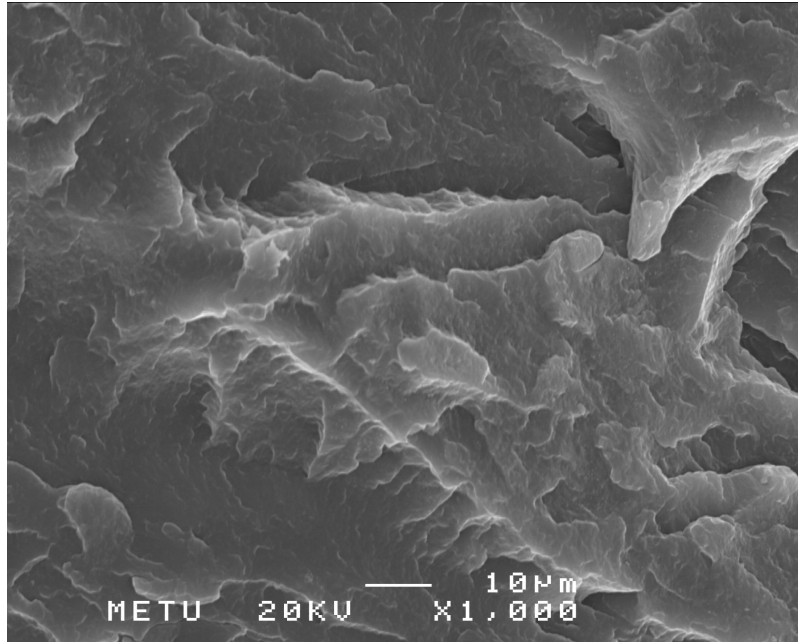
Figure 3.20 Fracture surface of 2 % PPy-PP composite
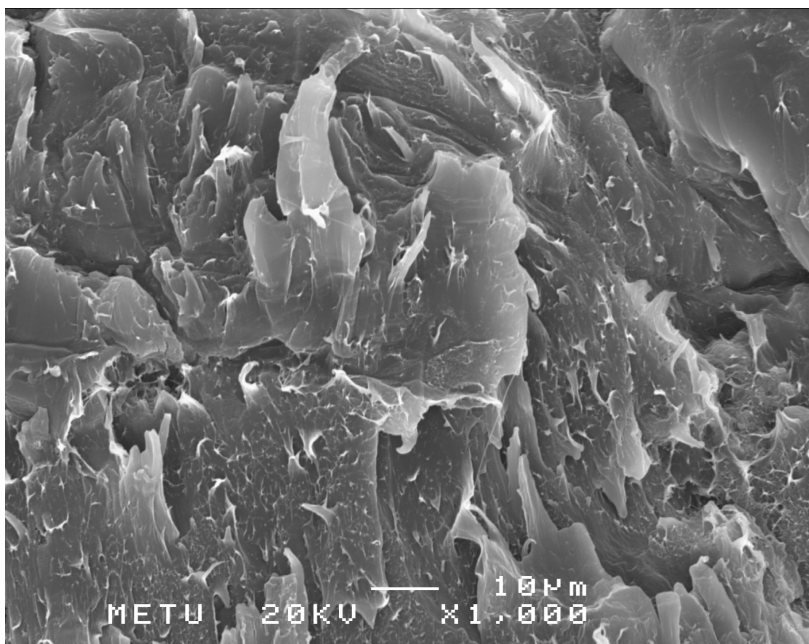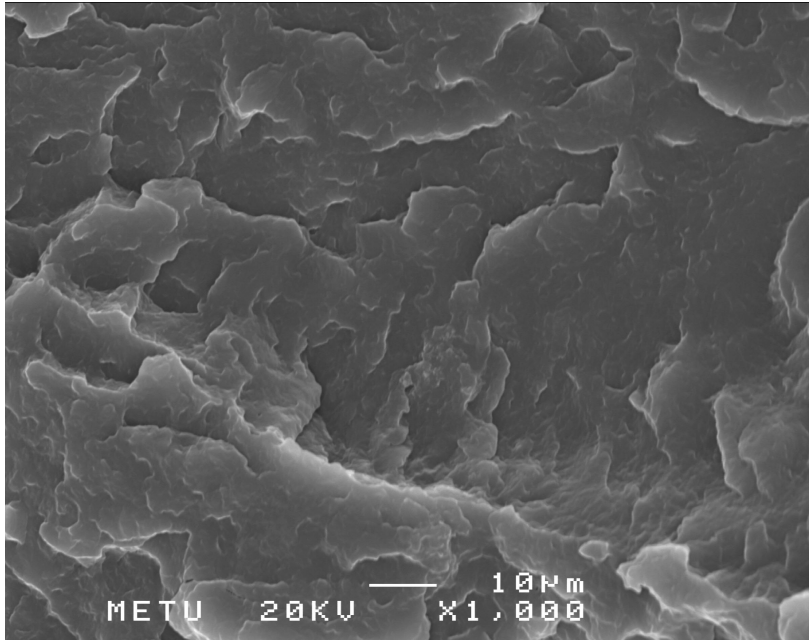
Figure 3.21 Fracture surface of 5 % PP-PPy composite
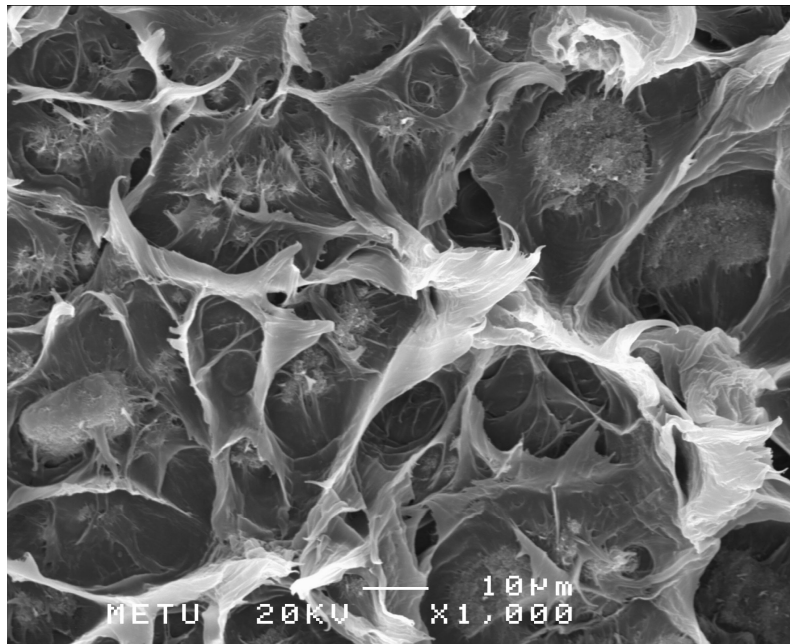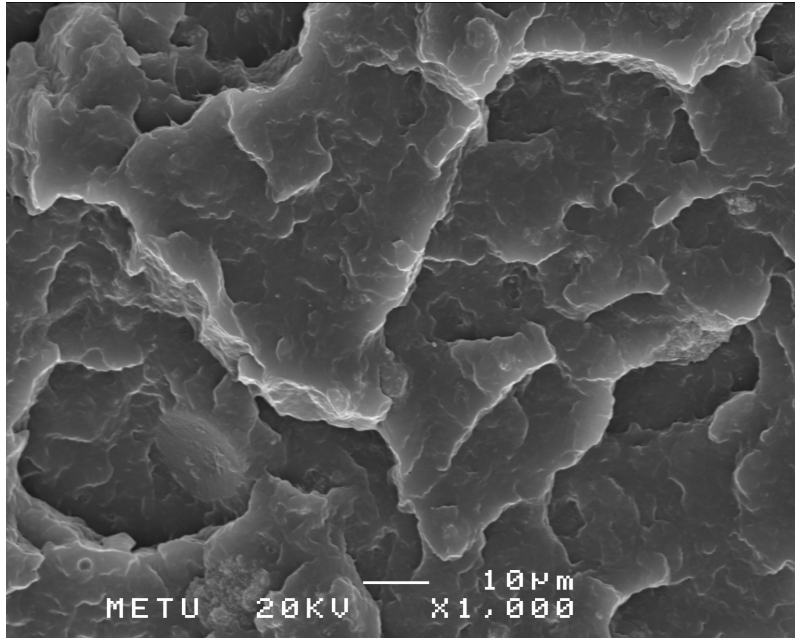
Figure 3.22 Fracture surface of 10 % PPy-PP composite
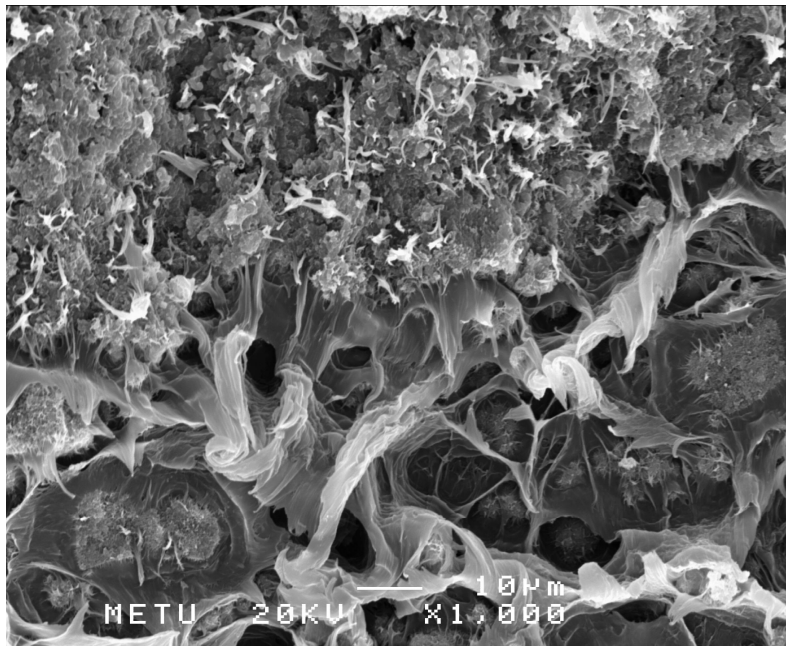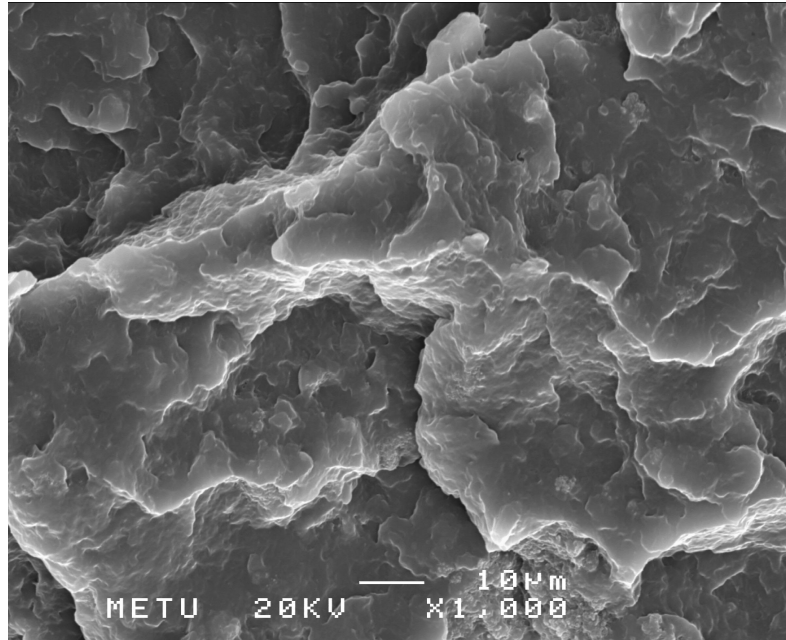
Figure 3.23 Fracture surface of 20 % PPy-PP composite

CHAPTER 4

CONCLUSIONS

Nanocomposites of polypyrrole (PPy) with nanodimensional organo-montmorillonite (OMMT) were prepared via *in situ* intercalation of pyrrole (Py) in the presence of ammonium persulfate as an oxidant dispersion of water solvent. In this method, a series of composites having composition ranging from 1 to 15 % by weight OMMT were synthesized.

FTIR spectra provide the intercalation of dodecylamine in the MMT layers and the modification of MMT was achieved. FTIR spectrum of the PPy/OMMT nanocomposites contains peaks coming from both OMMT and PPy which indicates that PPy was incorporated in composite systems

The wide angle X-ray diffraction pattern of MMT and OMMT clay showed that peaks in the direction of d(001) were 9.10^0 (d-spacing = 9.71 Å) and 8.05^0 (10.97 Å) respectively. So, the untreated MMT was modified by dodeclyamine and its basal spacing became larger. Also, the wide angle X-ray diffraction showed the insertion of PPy between the layers of OMMT as the nanoscale layer.

Electrical conductivity of PPy/OMMT composites were in the order of 10^{-3} S/cm. Increasing OMMT content resulted in a slight decrease in the conductivity of composites. This was expected because the OMMT component is not electronically conductive and the incorporating of MMT clay into PPy matrix contributes a smaller molecular weight, reflecting a lower electrical conductivity.

The TGA thermogram of PPy and PPy/clay nanocomposites showed that the thermal stability of nanocomposites are better than pure PPy and also the thermal stability of nanocomposites increases with increasing clay content in the PPy/clay system. Because PPy was completely burned at 800^0C, but as loading of OMMT content increased in nanocomposites, the remaning amount of composite materials also increases. Introduction of inorganic components into organic materials can improve their thermal stability, as the dispersed silicate layers hinder the permeability of volatile degradation products out of the material.

SEM micrographs show that MMT has flaky particles arranged into the form of spheres with irregular size and OMMT particles are similar but have smaller size spheres and partial rearrangement of MMT spheres by dodecylamine. SEM micrographs showed the modification of OMMT by PPy. Also, SEM results indicated that when the OMMT content became higher (10% and 15% respectively), PPy/OMMT nanocomposites showed wealthy and much larger compact-packing of crystalline domains.

Despite of its high conductivity and good thermal and oxidative stability, PPy has a lack of stability and a poor processability like many electroactive polymers. In order to improve the processability of PPy, efforts have been made to obtain composites which contain both PPy and PP. For the PP/PPy composites, addition of 2 wt % PPy to PP, resulted in a dramatic decrease in the tensile strain at break, and slightly decraese in tensile strength were seen. As increasing PPy content, tensile strain at break went on to decrease and tensile strength began to increase respectively. Also, increasing PPy content in composites results increase in Young's modulus of composites. Because extension of PP matrix is prevented by PPy acting as the reinforcing phase. Also, Increase in the PPy content in PP/PPy composites results in an increase in conductivity.

It is seen from the SEM images of 2 % and 5 % PP/PPy composites that they have smooth surfaces. As the PPy loading increases in composite system to 10% and 20%, PPy adhered to PP matrix and during tensile test the filler driven out of PP

matrix while PP matrix oriented along the draw direction. As the filler loading increases, the amount of polymer needed for complete coating decrease.

REFERENCES

[1] Evaristo Riande, R. Diaz-Calleja, Electrical Properties of Polymers, Marcel Dekker, New York, 576, 2004

[2] C.K. Chiang, C.R Fincher, Y.W. Park, A.J. Heeger, H. Shirakawa, F.J. Louis, S.C. Gau, A.G. MacDiarmid, Phys. Rev. Lett., 39, 578-580, 1977

[3] G.G. Wallace, G.M. Spinks, Conductive Electroactive Polymers, pp: 8,51,53,68, 2003

[4] D. Kumar, R.C. Sharma, Eur.Polym.J., Vol.34, pp:1053-1060, 1998

[5] H. Shirakawa, Handbook of Conducting Polymers, T.A. Skotheim, R.L. Elsenbaumer, Marcel Dekker, New York, 1998, pp.197,208

[6] D.L. Wise, G.E. Wnek, D.J. Trantolo, T.M. Cooper, J.D. Gresser, Electrical and Optical Polymer Systems, Marcel Dekker, 1998

[7] L. B. Groenendaal, F. Jonas, D. Freitag, H. Pielartzik, J. R. Reynolds, Advenced Materials, 12, 2000

[8] J. Margolis, Conductive Polymers and Plastics, Chapman and Hall, pp.33, 120, 121, 1989

[9] A. Barlow, Entone-OMI representative, 1997

[10] L. Alcacer, Conducting Polymers Special Applications, D. Reidel Publishing Company, pp.5, 192, 1987

[11] W. R. Salaneck D. T. Clark E. J. Samuelsen, Science and Application of Conducting Polymers, IOP Publishing, pp.52, 55, 135, 168, 1991

[12] J.L. Bredas, R.R. Chance, R.Silbey, Phys. Rev., Part B, 10, 1982

[13] J.L. Bredas, G.B. Street, Acct. Chem, 18, 1985

[14] M. E. Lyons, Electroactive Polymer Electrochemistry Part1 Fundamentals, Plenum Pres, 1984

[15] T. A. Skotheim, Handbook of Conducting Polymers, Vol 1&2, Marcel Dekker, New York, 1986.

[16] M. G. Kanatzidis, Chem. Eng. News, 68(49), 36, 1990

[17] C. K. Chiang, C. R. Fincher, Jr., Y. W. Park, A. J. Heeger, H. Shirakawa, E. J. Louis, A. G. MacDiarmid, Phys. Rev. Lett., pp.39, 1098, 1977

[18] C. K. Chiang, M. A. Druy, S. C. Gau, A. J. Heeger, E. J. Louis, A. G. MacDiarmid, J. Am. Chem. Soc., pp.100, 1013, 1978

[19] J.L. Bredas, B. Thelmans, J. M. Andre, R. R. Chance, R. Sibley, Synth. Met., 9, pp:265, 1984.

[20] L. Lauchan, S. Etamad, T.C. Chung, A.J. Heeger, A.G. MacDiarmid, Phys. Rev. B, 24, 1981,

[21] C.G. Wu, Y.R. Yeh, J.Y. Chen, Y.H. Chiou, Polymer, Vol. 42, 2001, pp: 2877-2885

[22] A.D. Pomogailo, V. N. Kestelman, Metallopolymer Nanocomposites, pp:321, 2006

[23] Mel. M. Schwartz, Composite Materials, New Jersey, Prentice Hall PTR, 1997

[24] M. G. Kanatzidis, C.-G. Wu, H. O. Marcy, D. C. DeGroot, J. L. Schindler, C. R. Kannewurf, M. Benz and E. LeGoff, "Crystalline Inorganic Hosts as Media for the Synthesis of Conductive Polymers" "Supramolecular Chemistry in Two and Three Dimensions" T. Bein Ed. ACS Symposium Series,pp. 499, 194-219, 1992

[25] J. Luo and I. M. Daniel, "Characterization and Modeling of Mechanical Behavior of Polymer/clay Nanocomposites", Comp. Sci. and Tech., vol.63, 1607-1616, 2003.

[26] Lamellar Polymer-LixMoO3 Nanocomposites Via Encapsulative Precipitation" Lei Wang, Jon Schindler, Carl R. Kannewurf, Mercouri G. Kanatzidis, J. Mater. Chem., 7, 1277-1283, 1997

[27] The Clay Mineral Group
http://www.galleries.com/minerals/silicate/clays.htm, last accessed on 4th July 2007

[28] The A to Z Nanotechnolgy
http://www.azom.com/details.asp?ArticleID=936, last accessed on 4th July 2007

[29] S.Yariv and H. Cross, Organo-Clay Complexes and Interactions, Marcel Dekker, New york, pp: 39-40, 84-87, 2002

[30] Sorptive Minerals Institute, Minerals&Ores
http://www.sorptive.org/pages/page02.html, last accessed on 4th July 2007

[31] Montmorillonite.
http://en.wikipedia.org/wiki/montmorillonite, last accessed on 4th July 2007

[32] P.C. LeBaron, Z. Wang And T.J Pinnavaia, "Polymer-layerd silicate nanocomposites: an overview", Applied Clay Science, vol.15, 11-29, 1999.

[33] Masami Okamoto, Polymer/Layered Silicate Nanocomposites, Rapra Technology Limited, United Kingdom, 2003

[34] C. Liu, T. Tang, Z.Zhao, B. Huang, J. Polym Sci, Part A: Polym Chem., 40, 1892, 2002

[35] S.C.Tjong, Nanocrystalline Materials: Their Synthesis Structure Property relationships and Applications, elsevıer, New york, pp: 323-324, 2006

[36] H. Chang, Y. Chunle, L. Yongfang, Synthetic Metals, pp 539, 2003

[37] K. Boukerma, Jean-Yves Piquemal, M. M. Chehimi, M. Mravcakova, M. Omastova, P. Beaunier, Synthesis and interfacial properties of montmorillonite/polypyrrole nanocomposites Polymer 47, pp: 569-576, 2005

[38] L.X. Wang, X.G. Li, Y.L. Yang, Reactive and Functional Polymers, Vol.47, pp: 125-139, 2001

[39] J.W. Kim, F. Liu, H.J. Choi, S.H. Hong, J. Joo, Intercalated polypyrrole/Na$^+$-montmorillonite nanocomposite via an inverted emulsion pathway method, Polymer 44, pp: 289-293, 2002

[40] H. Bai, Q.Chen, C. Li, C. Lu, G. Shi, Electrosynthesis of polypyrrole/sulfonated polyaniline composite films and their applications for ammonia gas sensing, Polymer 48, pp: 4015-4020, 2007

[41] Gaoyi Han and Gaoquan Shi, Porous polypyrrole/polymethylmethacrylate composite film prepared by vapor deposition polymerization of pyrrole and its application for ammonia detection, Thin Solid Films 515, pp: 6986–6991, 2007

[42] W.S. Barde, S.V. Pakade, S.P. Yawale, Ionic conductivity in polypyrrole-poly (vinyl acetate) films synthesized by chemical oxidative polymerization method, Journal of Non-Crystalline Solids 353, pp: 1460-1465, 2007

[43] Q. Cheng, V. Pavlinek, C. Li, Synthesis and structural properties of polypyrrole/nano-Y_2O_3 conducting composite, Applied Surface Science 253, pp: 1736-1740, 2006

[44] M.V. Murugendrappa, A. Parveen, M.V.N. Ambika Prasad, Synthesis, characterization and ac conductivity studies of polypyrrole-vanadium pentaoxide composites, Materials Science and Engineering A 459, pp: 371-374, 2007

[45] Suprakas SinhaRay and Mukul Biswas, Preparation and evaluation of composites from montmorillonite and some heterocyclic polymers: 3 a water dispersible nanocomposite from pyrrole-montmorillonite polymerization systems, Materials Research Bulletin, Vol. 34, pp: 1187-1194, 1999

[46] J.M. Yeh, C.P. Chin, S. Chang, Enhanced corrosion protection coatings prepared from soluble electronically conductive polypyrrole-clay nanocomposite materials, Journal of Applied Polymer Science, Vol. 88, pp: 3264-3272, 2003

[47] H.Q. Xie, C.M. Liu, J.S. Guo, Preparation of conductive polypyrrole composites by in-situ polymerization, Polym Int. 48, pp: 1099-1107, 1999

[48] Orica Limited, Polypropylene
http://www.pacia.org.au/_uploaditems/docs/3.polypropylene.pdf, last accessed on 4th July 2007

[49] San Diego Plastics Inc.
http://www.sdplastics.com/polypro.html, last accessed on 4th July 2007

[50] J.R. Fried, Polymer Science and Technology, Prentice Hall PTR, New Jersey, 1995

[51] Q.H.Zeng, D.Z.Wang, A.B.Yu, G.Q. Lu, Synthesis of polymer–montmorillonite nanocomposites by *in situ* intercalative polymerization, Nanotechnology,13, pp: 549-553, 2002

[52] J.M. Yeh, C.P. Chin, J. Appl. Polym. Sci. 88, pp:1072, 2003